

Ironing out the crease

Nadav Drukker^{*1} and Maxime Trépanier^{†2}

¹*Department of Mathematics, King's College London,
London, WC2R 2LS, United Kingdom*

²*Institute for Theoretical and Mathematical Physics (ITMP),
Moscow 119991, Russia*

Abstract

The crease is a surface operator folded by a finite angle along an infinite line. Several realisations of it in the 6d $\mathcal{N} = (2, 0)$ theory are studied here. It plays a role similar to the generalised quark-antiquark potential, or the cusp anomalous dimension, in gauge theories. We identify a finite quantity that can be studied despite the conformal anomalies ubiquitous with surface operators and evaluate it in free field theory and in the holographic dual. We also find a subtle difference between the infinite crease and its conformal transform to a compact observable comprised of two glued hemispheres, reminiscent of the circular Wilson loop. We prove by a novel application of defect CFT techniques for the $SO(2, 1)$ symmetry along the fold that the near-BPS behaviour of the crease is determined as the derivative of the compact observable with respect to its angle, as in the bremsstrahlung function. We also comment about the lightlike limit of the crease in Minkowski space.

^{*}nadav.drukker@gmail.com

[†]trepanier.maxime@gmail.com

Contents

1	Introduction and summary	1
2	Free theory	5
2.1	The spherical crease	5
2.2	The crease singularity	7
2.3	The infinite crease	8
3	Holography	9
3.1	The setup	9
3.2	BPS case	10
3.3	Non-BPS case	12
3.4	Near-BPS expansion	14
3.5	Antiparallel planes limit	15
4	Lightlike crease	16
4.1	Analytic continuation	17
4.2	Solutions in lorentzian AdS	18
4.3	Global solutions	19
5	Defect CFT	21
5.1	Near sphere expansion	22
5.2	Near-BPS expansion	23
6	Conclusion	26
A	Infinite crease in the Poincaré patch	28
A.1	Solution	28
A.2	Calibration equations	29

1 Introduction and summary

In order to make progress on the 6d $\mathcal{N} = (2, 0)$ theory we need to either find avatars of the theory with lagrangian descriptions or use whatever limited tools there are in the absence of a lagrangian to study the theory. For examples of recent attempts in the former approach, see e.g. [1–3]. Here instead we follow the latter approach, extending our programme [4–8] focused on the most natural observables on the theory—the 2d surface operators.

The simplest possible surfaces are the plane and sphere [9] which can preserve the maximal amount of residual supersymmetry, 16 supercharges, as well as conformal symmetry and overall the algebra $\mathfrak{osp}(4^*|2)^2$. Those are very natural starting points for exploring general surface operators, but contain little information on their own. The sphere suffers from a conformal anomaly so its expectation value depends on its radius R

$$\langle V_{S^2} \rangle \propto R^{4c-2a_1}, \tag{1.1}$$

where a_1 and c are the anomaly coefficients given below in (1.10).

One can view the plane as the worldsurface of an infinite straight string. A natural question is to evaluate the potential between two strings, or the plane-antiplane configuration, as was studied already in [10]. Amongst other things, in this paper we enrich this configuration by allowing each plane to associate to a different scalar field, which gives a continuous

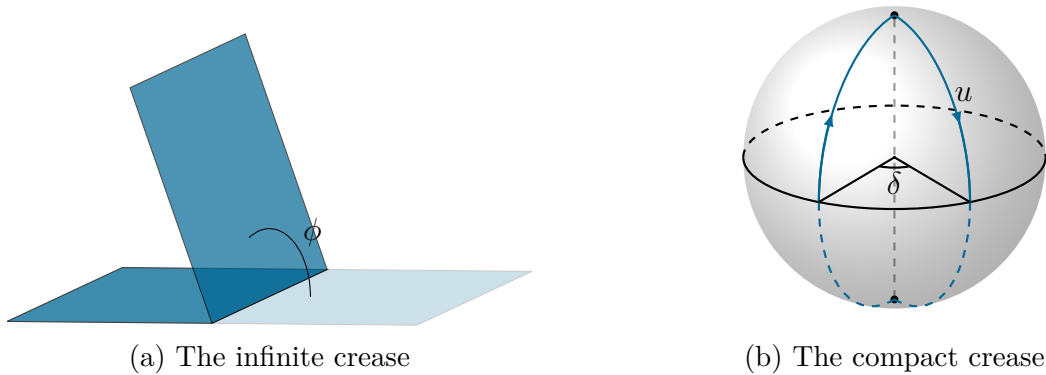


Figure 1: On the left, the infinite crease with $\phi = 2\pi/3$. On the right, a representation of the same crease after a conformal transformation. Each of the half planes is mapped to a hemisphere, here represented by the two arcs on S^2 (since we cannot draw S^3). Each point along the arc represents a circle, which shrinks at the equator ($z = 0$ in the image) and is of maximal radius 1 at the north pole, where it is also glued to the second hemisphere.

parameter θ interpolating between the anti-parallel planes with $\theta = 0$ and the BPS parallel planes at $\theta = \pi$.

A further generalisation of the system is the crease: two half-planes joined at an angle ϕ along a line (see figure 1). When $\phi = 0$ this is a single 1/2 BPS plane and when $\phi \rightarrow \pi$ it approaches the antiparallel planes.

This is a clear analogue of the cusped Wilson loop or “generalised quark-antiquark” system studied in [11–16]. Another natural 2d analogue of the cusp is a cone. Under a conformal transformation to $S^5 \times \mathbb{R}$ the cone becomes a cylinder which is a circle in S^5 extending along the \mathbb{R} direction. BPS versions of such operators were studied in [17] and the limit of a BPS cylinder in \mathbb{R}^6 in [8].

The crease configuration with the additional angle θ and several related surfaces are the subject of this paper. Our goal is to define and evaluate a meaningful physical quantity $U(\phi, \theta)$, analogous to the generalised quark-antiquark potential or cusp anomalous dimension. This quantity can be viewed as the potential between the two half planes, but on a more abstract level, it is a finite observable of the $\mathcal{N} = (2, 0)$ theory that can be (at least partially) evaluated. As we now have a good handle on the anomaly coefficients, we are behoven to find more refined quantities associated to surface operators and this is exactly such an observable.

In the remainder of the introduction we define the quantity $U(\phi, \theta)$ and discuss its salient features. We then proceed to evaluate it in the subsequent sections.

The observable we study has several realisations. First, as an infinite flat crease between two half-planes parametrised by $\tau, \sigma \in \mathbb{R}$

$$x^\mu = \begin{cases} (\tau, \sigma, 0, 0, 0, 0), & \sigma \leq 0, \\ (\tau, \sigma \cos \phi, \sigma \sin \phi, 0, 0, 0), & \sigma \geq 0. \end{cases} \quad (1.2)$$

The surface also breaks the R-symmetry. It is natural to have along each half-plane a uniform breaking, expressed by a unit 5-vector n^I as

$$n^I = \begin{cases} (1, 0, 0, 0, 0), & \sigma \leq 0, \\ (\cos \theta, \sin \theta, 0, 0, 0), & \sigma \geq 0. \end{cases} \quad (1.3)$$

The 1/2 BPS plane is clearly at $\theta = \phi = 0$. If $\theta = \pm\phi \neq 0$ this operator is 1/4 BPS and according to the classification of BPS surface operators in [7] it is of Type- \mathbb{R} , since it has translation invariance (it is also of Type- \mathbb{H} , which is utilised in Appendix A.2). For $\theta \neq \pm\phi$ no supersymmetry is preserved, but still in all cases the surface operator preserves the 1d conformal group $SO(2, 1)$, the transverse rotation group $SO(3)$ as well as $SO(3)$ R-symmetry. We refer to a surface operator with this geometry as an *infinite crease*.

Under a conformal transformation a plane is mapped to a sphere and a half-plane to a hemisphere. The crease is mapped into a pair of hemispheres inside S^3 joined along a large circle. Explicitly we can express $S^3 \subset \mathbb{R}^4$ as

$$\begin{aligned} x^1 &= R \cos u \cos v, & x^2 &= R \cos u \sin v, \\ x^3 &= R \sin u \cos w, & x^4 &= R \sin u \sin w, \end{aligned} \quad (1.4)$$

with $u \in [0, \pi/2]$ and $v, w \in [0, 2\pi)$. Each hemisphere is specified by a fixed w , which we take to be $w = \phi/2$ and $w = \pi - \phi/2$. They are clearly joined at an angle $\pi - \phi$ along the $u = 0$ circle. In the following we refer to this as the *spherical crease*.

Again we can associate to each of the hemispheres a different scalar coupling separated by an angle θ . A simple way to write it is by extending the domain of u to $[-\pi/2, \pi/2]$ with $x^4 = R \sin |u| \sin(\phi/2)$ and

$$n^1 = \cos \frac{\theta}{2}, \quad n^2 = \text{sign } u \sin \frac{\theta}{2}. \quad (1.5)$$

As with the infinite crease, when $\theta = \phi$ this is 1/4 BPS, but now it is not invariant under Poincaré supercharges but only combinations with special conformal transformations, making it of Type-S, in the classification of [7].

Translation invariance of the infinite crease suggests that any observable we calculate would be extensive in its length, but in fact any calculation preserving the conformal symmetry should be extensive in the area of the half-planes when endowed with a hyperbolic metric. It is thus natural to conformally transform \mathbb{R}^6 to $AdS_2 \times S^4$ as¹

$$\sum_{\mu=1}^6 dx^\mu dx^\mu = r^2 \left(\frac{dx^1 dx^1 + dr dr}{r^2} + d\Omega_4^2 \right), \quad r^2 = \sum_{\mu=2}^6 (x^\mu)^2. \quad (1.6)$$

The crease (1.2) is the union of two copies of AdS_2 at points on S^4 separated by the angle $\pi - \phi$. In this picture, the crease singularity is replaced by the jump at the boundary of the hyperbolic spaces.

Likewise for the spherical crease, if we start with the theory on \mathbb{R}^6 , stereographically project to $S^6 \subset \mathbb{R}^7$ given by (1.4) with $R = 1$ and the w circle extended to S^4 , we can rewrite the S^6 metric as

$$du^2 + \cos^2 u dv^2 + \sin^2 u d\Omega_4^2 = \frac{1}{\cosh^2 \rho} \left(d\rho^2 + \sinh^2 \rho dv^2 + d\Omega_4^2 \right). \quad (1.7)$$

This is accomplished with $\cosh \rho = 1/\sin u$.

The area of AdS_2 diverges so any quantity we evaluate should also suffer from those divergences. The natural regularisation of the area gives zero for the upper half plane model in (1.6) and -2π for the disc model in (1.7).

¹By AdS_2 we always mean Euclidean AdS_2 , i.e. \mathbb{H}_2 .

In the latter case we can therefore unambiguously define the potential $U(\phi, \theta)$ to be the density that arises in the calculation, such that when using the disc model of AdS_2 , the regularised expectation value of the spherical crease is $\exp[2\pi U(\phi, \theta)]$. In the case of the infinite crease, where the regularised area vanishes, we can still try to define the potential via the density, but it is more subtle, as it is multiplied by zero in the final expression.

There is one more subtlety though, which is the conformal anomaly arising in calculating surface operators. The expectation value of a general surface operator suffers from logarithmic divergences proportional to the integral of the anomaly density [18, 4]

$$\mathcal{A} = \frac{1}{4\pi} \left(a_1 \mathcal{R} + a_2 (H^2 + 4 \operatorname{tr} P) + b \operatorname{tr} W + c (\partial n)^2 \right), \quad (1.8)$$

where \mathcal{R} is the Ricci scalar of the induced metric h_{ab} on the surface, H^μ the mean curvature vector, $P = h^{ab} P_{ab}$ is the trace of the pullback of the Schouten tensor, W is the pullback of the Weyl tensor and ∂n is the gradient of the scalar coupling n^I . The prefactors are known as anomaly coefficients and are intrinsic properties of the theory and type of surface operator. It is known [6] that for this theory $b = 0$ and $c = -a_2$. In the abelian theory the coefficients are [4]

$$a_1^{(1)} = \frac{1}{2}, \quad c^{(1)} = \frac{1}{2}, \quad (1.9)$$

and for a surface operator in the fundamental representation in the nonabelian theory with algebra A_{N-1} they are [19–22]

$$a_1^{(N)} = \frac{1}{2} - \frac{1}{2N}, \quad c^{(N)} = N - \frac{1}{2} - \frac{1}{2N}. \quad (1.10)$$

The classical holographic calculation [19] just captures $a_1 \sim 0$ and $c \sim N$.

One may be concerned that all the creases that we study have an anomaly arising from the curvature singularity at the crease itself where H and ∂n have delta-function contributions. The formula (1.8) above does not apply for singular cases, and as we confirm in Section 2.2, indeed the singularity does not lead to an anomaly. Thus we see that the infinite crease has no anomaly and we can therefore try to define $U(\phi, \theta)$ as the potential density, but there is still the issue that its regularised integral vanishes. The spherical crease is anomalous, but since the anomaly is local and does not get a contribution from the crease singularity, it is independent of the angles, and the same as for the sphere with $\phi = \theta = 0$ and equal to $2a_1 - 4c$ (1.1) We then can define

$$U(\phi, \theta) = \frac{1}{2\pi} \left(\log \langle V_{\phi, \theta} \rangle - \log \langle V_{S^2} \rangle \right), \quad (1.11)$$

with the 2π factor arises from the area of the Poincaré disc.

It is most obvious that the anomaly does not depend on ϕ and θ in the $AdS_2 \times S^4$ picture. Here there are two disconnected AdS_2 factors with vanishing extrinsic curvature, so by the Gauss-Codazzi equation, the second fundamental form is twice the Ricci scalar, which is a constant -2 , so the anomaly density is $(a_1 + 2a_2)\mathcal{R}/4\pi$ which after integration (and with the appropriate boundary term) gives for each AdS_2 either zero or $a_1 - 2c$, depending on the topology.

Having defined $U(\phi, \theta)$ we proceed in the rest of the paper to evaluate it: First in the free abelian version of the $\mathcal{N} = (2, 0)$ theory in Section 2 and then in the holographic dual in terms of M2-branes in $AdS_7 \times S^4$ in Section 3. The results of the two calculations are

not identical, so this observable is an interesting quantity that depends on the rank of the algebra underlying the theory (as well as a representation of that algebra to which the surface operator is related) and ϕ and θ .

If we focus on the BPS case, when $\phi = \theta$ the expressions do not vanish, as one may have expected. Instead we find

$$U(\phi, \phi) = \frac{C}{\pi} \log \cos \frac{\phi}{2}. \quad (1.12)$$

In both the free theory and at leading order at large N , the constant C is the same as the anomaly coefficient c in (1.10). Interestingly, we find the same functional dependence on ϕ in both calculations.

Like in the recently studied cases of the torus and cylinder [8] or those in [17], this is a finite nonzero quantity associated to a BPS observable, similar in that regard to the circular Wilson loop in $\mathcal{N} = 4$ SYM in 4d [23–25].

This can be extended to the near-BPS limit, where

$$U(\phi, \theta) = \frac{C}{\pi} \log \cos \frac{\phi}{2} - \frac{C}{2\pi} (\phi - \theta) \tan \frac{\phi}{2} + \mathcal{O}((\phi - \theta)^2). \quad (1.13)$$

For small ϕ and θ , we can show that there is no $\phi\theta$ term and find

$$U(\phi, \theta) = -\frac{C}{8\pi} (2\phi^2 - \theta^2) + \dots \quad (1.14)$$

This expression is similar in spirit to the bremsstrahlung formula of [13, 26], which arises from the nearly straight cusped Wilson loop. The expression (1.13), which can also be written as

$$U(\phi, \theta) = \left(1 + (\phi - \theta) \frac{d}{d\phi} \right) U(\phi, \phi) + \mathcal{O}((\phi - \theta)^2), \quad (1.15)$$

is then akin to the “generalised bremsstrahlung formula” valid for near-BPS cusps in $\mathcal{N} = 4$ SYM. In Section 5 we reproduce these results from a defect CFT analysis and show that indeed $C = c$, the anomaly coefficient.

One more special example of the crease, when the two half-planes approach lightlike surfaces, is studied in Section 4. This is very similar to the case of the lightlike cusp [27] as well as its extension to the 4-cusp solution of Alday and Maldacena [28]. In our case the analogue of the 4-cusp solution involves 2 lightcones joined at a circular crease. We discuss some properties of those solutions and evaluate their action.

We comment about possible applications and extensions of this work in Section 6.

2 Free theory

2.1 The spherical crease

We start with the abelian version of the $\mathcal{N} = (2, 0)$ theory [29, 30]. The field content of the theory is

- $B_{\mu\nu}$, a two-form with self-dual field strength.
- Φ^I , five scalar fields.

- Ψ , eight symplectic Majorana fermions.

The surface operators of this theory are constructed explicitly in [4, 31]. They are built out of the fields B and Φ and are written as

$$V_{\phi,\theta} = \exp \int_{\Sigma} \sqrt{h} \left[\frac{i}{2} B_{\mu\nu} \partial_a x^\mu \partial_b x^\nu \varepsilon^{ab} - n^I \Phi^I \right] d^2\sigma. \quad (2.1)$$

Here a, b are the indices of the coordinates σ^a parametrising the surface; in our definition of the crease (1.4), we take $\sigma^a = (u, v)$. h_{ab} is the induced metric, ε^{ab} is the antisymmetric tensor normalised with a factor of $1/\sqrt{h}$ and n^I are the scalar couplings, which in our examples are given in (1.5).

Despite the subtleties related to the self-duality of B , one can derive propagators for the bosonic fields in flat space. Including a short distance regulator ϵ they are [32, 33, 31, 4]

$$\langle \Phi^I(x) \Phi^J(y) \rangle = \frac{\delta^{IJ}}{2\pi^2(|x-y|^2 + 2\epsilon^2)^2}, \quad (2.2a)$$

$$\langle B_{\mu\nu}(x) B_{\rho\sigma}(y) \rangle = \frac{\delta_{\mu\rho} \delta_{\nu\sigma} - \delta_{\mu\sigma} \delta_{\nu\rho}}{2\pi^2(|x-y|^2 + 2\epsilon^2)^2}. \quad (2.2b)$$

We can use these propagators to calculate the expectation value of the spherical crease. It is easy to show that because the theory is free, the expectation value is given by (the exponential of) the propagator integrated over 2 copies of the surface. There are two contributions, coming from integrating the propagator over two copies of the same hemisphere and the opposites hemispheres. Using the explicit parametrisation (1.4), (1.5), the log of the expectation value can be expressed as

$$\log \langle V_{\phi,\theta} \rangle = \frac{1}{2} \int R^4 \cos u \cos u' du dv du' dv' (2\Delta_{\pi,\pi}(u, v; u', v') + 2\Delta_{\phi,\theta}(u, v; u', v')) , \quad (2.3)$$

where the combined propagator is

$$\Delta_{\phi,\theta}(u, v; u', v') = \frac{1}{8\pi^2 R^4} \frac{\cos \theta - \cos u \cos u' \cos(v-v') \cos \phi + \sin u \sin u'}{(1 - \cos u \cos u' \cos(v-v') + \sin u \sin u' \cos \phi + \epsilon^2/R^2)^2}. \quad (2.4)$$

We can perform the v and v' integral using equation (2.554) of [34]

$$\int_0^{2\pi} dv dv' \frac{A + B \cos(v-v')}{(a + b \cos(v-v'))^2} = 2\pi \int_0^{2\pi} dv \frac{A + B \cos v}{(a + b \cos v)^2} = 4\pi^2 \frac{aA - bB}{[a^2 - b^2]^{3/2}}, \quad a > b. \quad (2.5)$$

With the appropriate A , B , a and b and replacing $s = \sin u$ and $s' = \sin u'$ this is (with $R = 1$)

$$\begin{aligned} \int dv dv' \Delta_{\phi,\theta} &= \frac{1}{2} \frac{(\cos \theta - \cos \phi)(1 + \epsilon^2 - ss' \cos \phi)}{[(1 + \epsilon^2 + ss' \sin \phi)^2 - (1 - s^2)(1 - s'^2)]^{3/2}} \\ &\quad + \frac{1}{2} \frac{\cos \phi(s^2 + s'^2 + \epsilon^2) + ss'(1 + \epsilon^2 + \cos^2 \phi)}{[(1 + \epsilon^2 + ss' \sin \phi)^2 - (1 - s^2)(1 - s'^2)]^{3/2}}. \end{aligned} \quad (2.6)$$

Integrating this gives

$$\int ds dv ds' dv' \Delta_{\phi,\theta} = (\cos \theta - \cos \phi) \left[\frac{R\phi}{2^{3/2} \epsilon \sin \phi} - \frac{1}{4 \cos^2(\phi/2)} \right] + \log \left(2 \cos \frac{\phi}{2} \right) + \mathcal{O}(\epsilon). \quad (2.7)$$

The contribution from two copies of the same hemisphere, for which $\phi = \theta = \pi$, has further UV divergences and we cannot rely on the regularised result of the integral above. Instead, after subtracting ϵ^2 from the numerator in (2.4) we find that (2.6) is now

$$\int dv dv' \Delta_{\pi,\pi} = \frac{1}{2\sqrt{\epsilon^4 + 2\epsilon^2(1 - ss') + (s - s')^2}}, \quad (2.8)$$

and

$$\int ds dv ds' dv' \Delta_{\pi,\pi} = -\log \frac{\sqrt{2}\epsilon}{R} + \mathcal{O}(\epsilon). \quad (2.9)$$

Combining with (2.7) and removing the linear divergence we find

$$\log \langle V_{\phi,\theta} \rangle = \log \frac{\sqrt{2} R \cos(\phi/2)}{\epsilon} + \frac{\cos \phi - \cos \theta}{4 \cos^2(\phi/2)} + \mathcal{O}(\epsilon). \quad (2.10)$$

Setting $\phi = \theta = 0$ indeed reproduces the result for the sphere (1.1) with the anomaly coefficients (1.9).

We can then take the difference to the regular sphere case to read off the potential (1.11)

$$U^{(1)}(\phi, \theta) = \frac{1}{2\pi} \log \cos \frac{\phi}{2} + \frac{\cos \phi - \cos \theta}{8\pi \cos^2(\phi/2)}. \quad (2.11)$$

2.2 The crease singularity

In the above derivation we found a linear R/ϵ divergence. More confusing is the relation of this result to the anomaly formula (1.8). Along either the infinite or the compact crease, the mean curvature vector H has a delta function singularity, invalidating the formula. One may worry that under regularisation we would get a term similar to $\epsilon^{-1} \log \epsilon$, which we did not find above. We examine this apparent contradiction here.

For simplicity we choose to analyse the case of the sphere $\phi = 0$ with $\theta \neq 0$. n^I is given in (1.5) and clearly is singular at $u = 0$; we can regularise it by replacing the step function $\text{sign}(u)$ by a continuous function $f_l(u)$ with a regulator l . We can take for instance

$$f_l(u) = \begin{cases} u/l, & -l \leq u \leq l, \\ \text{sign}(u), & \text{otherwise.} \end{cases} \quad (2.12)$$

As $l \rightarrow 0$ this reduces to the step function.

It is easy to check that now $|\partial n| \sim 1/l$ for $|u| \leq l$ and the anomaly formula indeed gives a $l^{-1} \log \epsilon$ divergence. Any other regulator f_l would give the same behaviour up to a numerical factor.

The mechanism by which this discrepancy is resolved is easy to understand in this example. Using (2.4), the expectation value for the regularised crease in the free theory is

$$\frac{1}{16\pi^2} \int \cos u \cos u' du dv du' dv' \frac{n^I(u)n^I(u') - \cos u \cos u' \cos(v - v') - \sin u \sin u'}{(1 - \cos u \cos u' \cos(v - v') - \sin u \sin u' + \epsilon^2/R^2)^2}. \quad (2.13)$$

Instead of evaluating the exact expression, we expand in a power series in θ . For $\theta = 0$ this is the regular sphere, so there is no singularity, only the usual $-\log \epsilon$ anomaly. The

first nontrivial term is of order θ^2 and it is enough to capture the $l^{-1} \log \epsilon$ divergence. After expanding, the v, v' integrals are performed as before and substituting again $s = \sin u$ and $s' = \sin u'$ we are left with

$$-\frac{1}{32} \int_{-1}^1 ds ds' \frac{(1 - ss')(f_l(s) - f_l(s'))^2}{((s - s')^2 + (1 - ss')\epsilon^2 + \epsilon^4)^{3/2}}. \quad (2.14)$$

This integral can be performed and expanding the result first in ϵ with fixed l and then expanding in small l gives

$$\frac{1}{16l} + \frac{1}{8l} \log \frac{\epsilon}{4l} + \text{finite}. \quad (2.15)$$

For fixed l and $\epsilon \rightarrow 0$ we indeed find the result $l^{-1} \log \epsilon$ predicted by the anomaly formula. The $1/l$ and $l^{-1} \log l$ terms are then regarded as finite contributions.

But this expression does not lead to a $\epsilon^{-1} \log \epsilon$ divergence, as when we take $l \rightarrow \epsilon$, the $\log l$ compensates for the $\log \epsilon$ and all we are left with is a linear divergence $1/l \rightarrow 1/\epsilon$, in agreement with the explicit calculations. Furthermore, there are no new $\log \epsilon$ terms for $l \sim \epsilon$, and all the anomaly for the sphere with $\theta \neq 0$ is the same as the usual sphere, as indeed we found in (2.10).

Of course in this example we only look at the term of order θ^2 for a simple choice of f_l . We did not calculate the regularised crease for any ϕ and θ but we expect the same mechanism to reconcile the anomaly formula prediction with the results for the singular crease. Indeed ϵ in the logarithm must appear with some other scale, and the scale relevant for the singularity is l .

The observation that the crease does not give additional $\log^2 \epsilon$ or $\log \epsilon$ divergences was also made in the context of holographic entanglement entropy in [35–37].

2.3 The infinite crease

We defined the potential (1.11) in terms of the spherical crease and in all our calculations it is identical also to its AdS_2 realisation. Here we examine what can be calculated for the infinite crease.

Repeating the calculation with this geometry, the interesting contribution comes from propagators between different half-planes in (1.2). Using (2.2a), (2.2b) it reads

$$\log \langle V_{\phi, \theta}^{\text{inf}} \rangle = \frac{\cos \theta - \cos \phi}{2\pi^2} \int_{-\infty}^{\infty} d\tau d\tau' \int_0^{\infty} \frac{d\sigma d\sigma'}{[(\tau - \tau')^2 + (\sigma - \sigma')^2 + 4\sigma\sigma' \cos^2(\phi/2) + 2\epsilon^2]^2}. \quad (2.16)$$

Performing the integrals over τ', σ' and σ , we obtain

$$\log \langle V_{\phi, \theta}^{\text{inf}} \rangle = \frac{\cos \theta - \cos \phi}{2^{3/2} \pi \sin \phi} \phi \int_{-\infty}^{\infty} \frac{d\tau}{\epsilon}. \quad (2.17)$$

The resulting integral gives the overall length L/ϵ , which as a linear divergence can be removed. But we wish to view it instead as the volume of AdS_2 in the Poincaré patch

$$\int_{-\infty}^{\infty} \frac{d\tau}{\epsilon} = \int_{-\infty}^{\infty} d\tau \int_{\epsilon}^{\infty} \frac{d\sigma}{\sigma^2}. \quad (2.18)$$

Then we view the prefactor in (2.17) as representing the potential between the two planes

$$U_{\phi,\theta}^{\text{inf}} = \frac{\cos \theta - \cos \phi}{2^{3/2}\pi \sin \phi} \phi, \quad (2.19)$$

where we did not divide by $1/2\pi$ as in (1.11), since here we divide by the divergent area of the upper half plane instead of the finite regularised area of the Poincaré disc.

Interestingly, the answer is different from the case of the spherical crease (2.11), and here it vanishes in the BPS case $\phi = \theta$. Also, it has the same functional form as the cusped Wilson loop in $\mathcal{N} = 4$ SYM at one-loop order [12].

A naive integration of (2.16) without the ϵ regulator is clearly divergent. But for fixed σ and τ one can perform the full σ', τ' integral to find

$$\frac{\cos \theta - \cos \phi}{8\pi \cos^2(\phi/2)}, \quad (2.20)$$

which is now the same as (2.11) except for the $1/(2\pi) \log \cos(\phi/2)$ term. The remaining τ, σ integrals are as in (2.18).

These two calculations are consistent with using two different cutoffs ϵ and ϵ' related by

$$\epsilon = \frac{2^{3/2} \cos^2(\phi/2) \phi}{\sin \phi} \epsilon'. \quad (2.21)$$

Note that to reproduce the missing term from (2.11), we would need to include a θ dependence in cutoff, which is not very natural as a field theory cutoff. So we conclude that the result is rather ambiguous and scheme dependent, but in any case vanishes in the BPS case.

We look at the holographic dual of the infinite crease in Appendix A and find similar ambiguities.

3 Holography

3.1 The setup

The spherical crease is inside S^3 and involves two scalar fields. It can therefore be described by an M2-brane inside $AdS_4 \times S^1 \subset AdS_7 \times S^4$. Writing the AdS_4 factor as an $AdS_2 \times S^1$ foliation, this is

$$ds^2 = 4L^2 \left[d\nu^2 + \cosh^2 \nu (d\rho^2 + \sinh^2 \rho dv^2) + \sinh^2 \nu d\varphi^2 \right] + L^2 d\vartheta^2. \quad (3.1)$$

Defining $\sinh \nu = 1/t$ the metric becomes

$$ds^2 = \frac{4L^2}{t^2} \left[\frac{dt^2}{1+t^2} + (1+t^2)(d\rho^2 + \sinh^2 \rho dv^2) + d\varphi^2 \right] + L^2 d\vartheta^2. \quad (3.2)$$

The M2-brane can be parametrised by the coordinates of AdS_2 : ρ, v , and in addition t . Because the crease has AdS_2 symmetry, we look for brane embeddings depending only on t , so we should solve for $\varphi(t)$ and $\vartheta(t)$. This description is not single valued; $\varphi(t)$ and $\vartheta(t)$ have two branches corresponding to each hemisphere of the spherical crease. At the boundary of

AdS ($t \rightarrow 0$), φ and ϑ should approach their asymptotic values (shifted to be symmetric around $\pi/2$ and 0)

$$\varphi(0) = \phi/2, \quad \pi - \phi/2, \quad \vartheta(0) = \pm\theta/2. \quad (3.3)$$

A single branch of the solution has $t \in (0, t_{\max}]$ and both branches meet at t_{\max} (see for example Figure 2)

$$\varphi(t_{\max}) = \pi/2, \quad \vartheta(t_{\max}) = 0. \quad (3.4)$$

The action is

$$S_{M2} = 8T_{M2}L^3 \int \sinh \rho \, d\rho \, dv \, dt \frac{1+t^2}{t^3} \sqrt{\frac{1}{1+t^2} + \varphi'^2 + \frac{t^2}{4}\vartheta'^2}. \quad (3.5)$$

Here T_{M2} is the M2-brane tension, which by the AdS/CFT dictionary [38] is $N/4\pi L^3$.

This lagrangian has two conserved quantities: the canonical momenta conjugate to φ and ϑ

$$J_\varphi = \frac{(1+t^2)\varphi'}{t^3 \sqrt{\frac{1}{1+t^2} + \varphi'^2 + \frac{t^2}{4}\vartheta'^2}}, \quad J_\vartheta = \frac{(1+t^2)\vartheta'}{4t \sqrt{\frac{1}{1+t^2} + \varphi'^2 + \frac{t^2}{4}\vartheta'^2}}. \quad (3.6)$$

Inverting these relations gives the first order equations of motion

$$\begin{aligned} \vartheta'(t) &= \frac{4J_\vartheta t}{\sqrt{(1+t^2)(1+2t^2 + (1-4J_\vartheta^2)t^4 - J_\varphi^2 t^6)}}, \\ \varphi'(t) &= \frac{J_\varphi t^3}{\sqrt{(1+t^2)(1+2t^2 + (1-4J_\vartheta^2)t^4 - J_\varphi^2 t^6)}}. \end{aligned} \quad (3.7)$$

In order for the brane to be smooth, we need that at t_{\max} both $\varphi', \vartheta' \rightarrow \infty$ together. This determines t_{\max} as one of the roots of the polynomial in the denominator of (3.7). More precisely, because both J_φ and J_ϑ are real, it is simple to show that the polynomial only has a single positive root. It can be factorised as

$$1 + 2t^2 + (1 - 4J_\vartheta^2)t^4 - J_\varphi^2 t^6 = -J_\varphi^2 (t^2 - \tau_1)(t^2 - \tau_2)(t^2 - t_{\max}^2). \quad (3.8)$$

The roots τ_1, τ_2 can be expressed explicitly in terms of J_φ, J_ϑ using the cubic formula, but we leave them implicit. They are either complex or real and negative. The root t_{\max} is real and positive.

3.2 BPS case

As we show in Appendix A.2, in the BPS case, the set of equations obtained in [7] relate the two momenta

$$2J_\vartheta = \pm J_\varphi, \quad (3.9)$$

or equivalently $\vartheta' = \pm 2\varphi'/t^2$. On the first branch, we expect φ to be monotonously increasing and ϑ to be decreasing, and because their derivatives are proportional to the conserved momenta (3.7), we should take the solution with the negative sign.

In particular this means that the polynomial appearing in the denominator of (3.7)

$$(1+t^2) \left[(1+t^2)^2 - (4J_\vartheta^2 + J_\varphi^2 t^2)t^4 \right], \quad (3.10)$$

has degenerate roots at $t^2 = -1$ and simplifies to

$$(1 + t^2)^2 (1 + t^2 - J_\varphi^2 t^4). \quad (3.11)$$

The factorisation of an additional factor of $1 + t^2$ implies that in this case, the equations of motion (3.7) contain the square root of a quadratic polynomial, so their solution is trigonometric, rather than elliptic.

Comparing with (3.8), we find a simple expression for t_{\max}

$$t_{\max}^2 = \frac{1 + \sqrt{1 + 4J_\varphi^2}}{2J_\varphi^2}. \quad (3.12)$$

Integrating ϑ' in (3.7) and imposing the boundary conditions (3.4) at t_{\max} , we obtain

$$\vartheta = \arctan \left(\frac{2J_\varphi \sqrt{1 + t^2 - J_\varphi^2 t^4}}{1 + (1 + 2J_\varphi^2)t^2} \right), \quad (3.13)$$

and similarly for φ

$$\varphi = \vartheta + \arcsin \left(\frac{J_\varphi t^2}{\sqrt{1 + t^2}} \right). \quad (3.14)$$

We can read the value of ϕ , θ from the solution by setting $t = 0$: (3.14) gives $\phi = \theta$ as expected (the case $\phi = -\theta$ is obtained by picking the positive sign in (3.9) instead), and (3.13) expresses J_φ in term of the angle ϕ

$$J_\varphi = \frac{1}{2} \tan \frac{\phi}{2}. \quad (3.15)$$

Finally, with these solutions in hand we can evaluate the action (3.5). The integral over AdS_2 diverges but is regularised to -2π . Using the equations of motion and the BPS condition (3.9), the action reduces to

$$S_{M2} = \frac{4N}{\pi} (-2\pi) \int_\epsilon^{t_{\max}} \frac{(1 + t^2) dt}{t^3 \sqrt{1 + t^2 - J_\varphi^2 t^4}}. \quad (3.16)$$

The integral over t gives

$$-\frac{\sqrt{1 + t^2 - J_\varphi^2 t^4}}{2t^2} - \frac{1}{4} \operatorname{arctanh} \frac{2\sqrt{1 + t^2 - J_\varphi^2 t^4}}{2 + t^2}. \quad (3.17)$$

This vanishes at $t = t_{\max}$. At $t = \epsilon$ the first term gives an ϵ^{-2} divergence corresponding to the usual area divergence; it can be safely discarded (or removed by an appropriate counterterm). The second term gives an important $\log \epsilon$ divergence

$$\begin{aligned} S_{M2} &= -2N \operatorname{arctanh} \left(1 - \frac{1}{8}(1 + 4J_\varphi^2)\epsilon^4 + \dots \right) = N \log \frac{(1 + 4J_\varphi^2)\epsilon^4}{16} + \dots \\ &= N \log \frac{\epsilon^4}{16 \cos^2(\phi/2)} + \dots \end{aligned} \quad (3.18)$$

Note that the coefficient of $\log \epsilon$ matches the expected conformal anomaly for the sphere $4N + \mathcal{O}(N^0) = 4c_1 - 2a_2$ (1.10). It must also appear in the form of $\log \epsilon/R$, and reproduces the expected behavior (1.1). Subtracting the action for the sphere then gives a finite quantity, from which we can read the BPS potential

$$U^{(N)}(\phi, \phi) = \frac{N}{\pi} \log \cos \frac{\phi}{2}. \quad (3.19)$$

3.3 Non-BPS case

For generic J_φ and J_ϑ , the equations of motion (3.7) can be brought into canonical elliptic form by performing the change of variables

$$y^2(t) = \frac{(t_{\max}^2 - t^2)(1 + \tau_2)}{(t_{\max}^2 - \tau_2)(1 + t^2)}, \quad (3.20)$$

after which the equations are

$$\begin{aligned} d\vartheta &= \frac{4J_\vartheta}{J_\varphi \sqrt{(t_{\max}^2 - \tau_1)(1 + \tau_2)}} \frac{dy}{\sqrt{(1 - y^2)(1 - y^2/y^2(\tau_1))}}, \\ d\varphi &= -\frac{1}{\sqrt{(t_{\max}^2 - \tau_1)(1 + \tau_2)}} \frac{dy}{\sqrt{(1 - y^2)(1 - y^2/y^2(\tau_1))}} \left[1 - \frac{(1 + \tau_2)(1 + t_{\max}^2)}{1 + \tau_2 - (\tau_2 - t_{\max}^2)y^2} \right]. \end{aligned} \quad (3.21)$$

These match the definition of elliptic integrals of the first and third kind

$$\begin{aligned} \mathbf{F}(\psi|k^2) &= \int_0^{\sin \psi} \frac{dy}{\sqrt{(1 - y^2)(1 - k^2y^2)}}, \\ \mathbf{\Pi}(n; \psi|k^2) &= \int_0^{\sin \psi} \frac{dy}{(1 - ny^2)\sqrt{(1 - y^2)(1 - k^2y^2)}}. \end{aligned} \quad (3.22)$$

The parameters appearing in their definition can be read from above, they are

$$\psi = \arcsin \sqrt{\frac{(t_{\max}^2 - t^2)(1 + \tau_2)}{(t_{\max}^2 - \tau_2)(1 + t^2)}}, \quad k^2 = \frac{(t_{\max}^2 - \tau_2)(1 + \tau_1)}{(t_{\max}^2 - \tau_1)(1 + \tau_2)}, \quad n = \frac{\tau_2 - t_{\max}^2}{1 + \tau_2}. \quad (3.23)$$

Imposing the gluing condition (3.4), we obtain

$$\vartheta(t) = -\frac{4J_\vartheta}{J_\varphi} \frac{\mathbf{F}(\psi|k^2)}{\sqrt{(t_{\max}^2 - \tau_1)(1 + \tau_2)}}, \quad \varphi(t) = \frac{\pi}{2} + \frac{\mathbf{F}(\psi|k^2) - (1 + t_{\max}^2)\mathbf{\Pi}(n; \psi|k^2)}{\sqrt{(t_{\max}^2 - \tau_1)(1 + \tau_2)}}. \quad (3.24)$$

At $t = t_{\max}$, the elliptic integrals vanish ($\psi = 0$), so the boundary conditions are manifestly respected.

What is not manifest in these expressions is that φ and ϑ are real functions. The behavior of the roots τ_1, τ_2 are captured by the discriminant, they are real and negative if

$$J_\varphi^2 \leq -\frac{2}{27} \left[1 - 36J_\vartheta^2 - (1 + 12J_\vartheta^2)^{3/2} \right], \quad (3.25)$$

which in particular includes the BPS case $J_\varphi = \pm 2J_\vartheta$, otherwise they are complex conjugate. When they are real, taking $\tau_1 < \tau_2$ makes all the quantities real, including φ, ϑ . When they are complex conjugate, exchanging τ_1 and τ_2 is a symmetry so φ and ϑ must be real as well.

Evaluating (3.24) at $t = 0$ relates ϕ and θ to J_φ and J_ϑ , but unlike the BPS case, these relations cannot be inverted in terms of fundamental functions. Instead we do this perturbatively below around $\phi = \theta$ (near-BPS limit) and around $\phi \sim \pi$ and $\theta = 0$ (antiparallel limit). Of course, it can also be done numerically as in Figure 2.

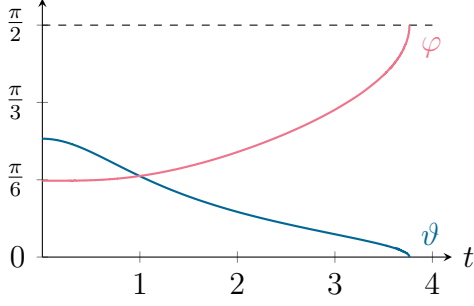


Figure 2: Example of solution to the equations of motion (3.7) for $\phi = \pi/3$ and $\theta = \pi/2$. $\vartheta(t)$ and $\varphi(t)$ are given analytically in (3.24), they depend on the parameters $J_\varphi = 0.262$, $J_\vartheta = -0.210$ which are found numerically. In this example $t_{\max} = 3.76$.

We now turn to calculating the action. Using the equations of motion (3.7) and again regularising the volume of AdS_2 , the action (3.5) reduces to

$$S_{M2} = \frac{4N}{\pi} (-2\pi) \int_\epsilon^{t_{\max}} \frac{(1+t^2)^{3/2} dt}{t^3 \sqrt{(1+t^2)^2 - 4J_\vartheta^2 t^4 - J_\varphi^2 t^6}}. \quad (3.26)$$

Using the change of variables (3.20), it too can be expressed in terms of elliptic integrals

$$\int \frac{dy}{(1-n'y^2)^2 \sqrt{(1-y^2)(1-k^2y^2)}} = \frac{n'^2 y \sqrt{(1-y^2)(1-k^2y^2)}}{1-n'y^2} \frac{1}{2(k^2-n')(n'-1)} \quad (3.27)$$

$$- \frac{n' \mathbf{E}(\psi|k^2) + (k^2-n') \mathbf{F}(\psi|k^2) + (n'(n'-2) + k^2(2n'-3)) \mathbf{\Pi}(n'; \psi|k^2)}{2(k^2-n')(1-n')},$$

where $n' = 1/y^2(0)$ differs from n in (3.23) and \mathbf{E} is the elliptic integral of the second kind

$$\mathbf{E}(\psi|k^2) = \int_0^{\sin \psi} dy \sqrt{\frac{1-k^2y^2}{1-y^2}}. \quad (3.28)$$

At $t = 0$ both the first term and $\mathbf{\Pi}$ diverge. This is the same divergence we encountered in the BPS case (3.18): to see it, it is easier to go back to (3.26) and expand for small t , which gives

$$-8N \int_\epsilon^{t_{\max}} \frac{dt}{t^3} \left[1 + \frac{t^2}{2} + \mathcal{O}(t^4) \right] = -8N \left[\frac{1}{2\epsilon^2} - \frac{1}{2} \log \epsilon \right] + \text{finite}. \quad (3.29)$$

Notice that both terms are independent of J_ϑ , J_φ , so they are independent of the angles and do not contribute to the potential $U(\phi, \theta)$.

The rest of the integral (3.27) is UV finite and calculates the potential $U(\phi, \theta)$ (up to the prefactor $4N/\pi$). The dependence on the angles is implicit, since all the variables and roots of the cubic polynomial (3.8) depend on J_φ , J_ϑ , and these are related to ϕ , θ by imposing the boundary conditions at $t = 0$ on the solution (3.24).

It is easy to evaluate the potential for specific ϕ and θ numerically, as in Figure 3.

The analysis thus far restricted to solutions with $0 < \vartheta < \theta/2$, but there are solutions that are multiply wound around the S^1_ϑ circle, where for each branch of the solution $0 < \vartheta < \pi n + \theta/2$, see for instance Figure 4. Those solutions can be described analytically, but they also arise when searching numerically for J_φ , J_ϑ .

We should compare their action to that of the unwound solution. They all have the same behaviour and divergence at small t , which is removed by the same counterterm. Looking at

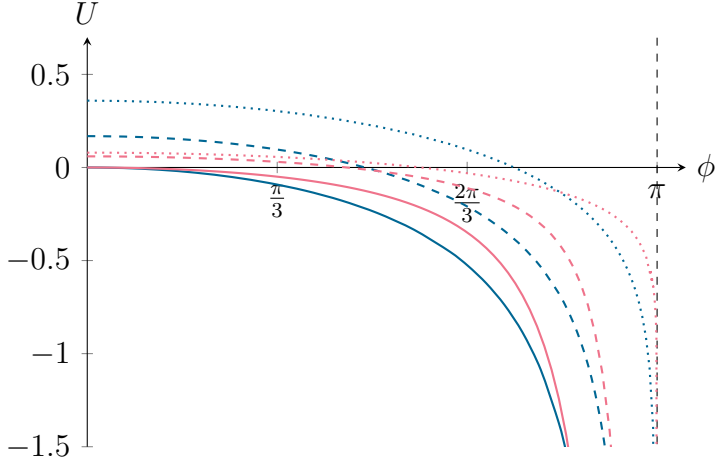


Figure 3: In blue, the potential $U(\phi, \theta)/N$ at large N obtained numerically from (3.26) for different values of θ : $\theta = 0$ (solid), $2\pi/3$ (dashed) and π (dotted). Notice the divergence near $\phi = \pi$, which is captured by the antiparallel planes limit (3.41). The potential at $N = 1$ for the same values of θ (2.11) is in red.

the action density, the difference between the solutions with different windings is finite, so they can be viewed as instantonic corrections. But it is more appropriate to treat the entire brane including the factor of the area of AdS_2 in the action (3.5). One may be tempted to replace the area by -2π as in (3.26), but this is inconsistent. Firstly, this amounts to different subtractions for different solutions, so does not form a consistent regularisation scheme. Furthermore, because of the negative sign, the more the solution is wound, the more dominant it would be. If we are to use a consistent regularisation scheme that renders the unwound solution finite, the wound solutions have infinite action and are therefore infinitely suppressed.

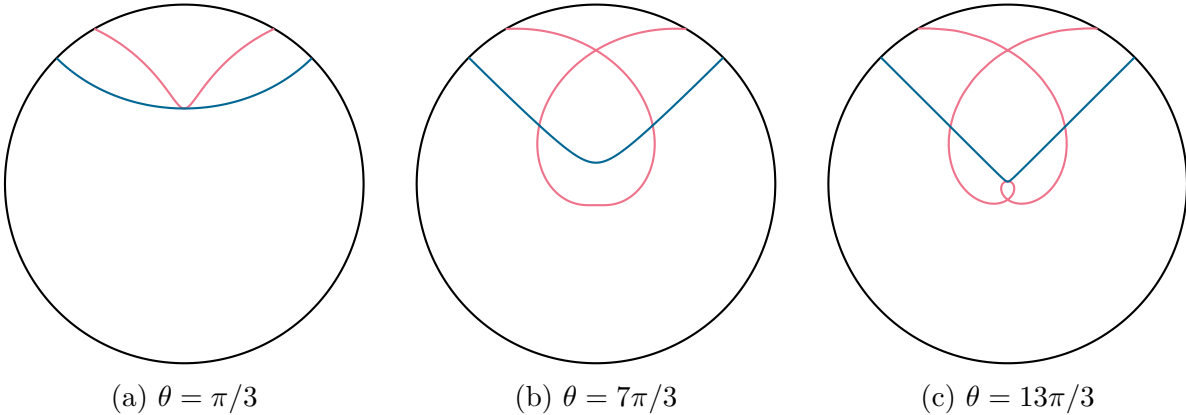


Figure 4: Example of solutions to the equations of motion with nontrivial windings for $\phi = \pi/2$ and $\theta = (\pi/3 \bmod 2\pi)$. The radial direction is $(1 + t^2)^{-1/2}$, with the black circle corresponding to the conformal boundary. The blue curve is $\varphi(t)$ and the red curve is $\vartheta(t)$.

3.4 Near-BPS expansion

Here we study the solutions in a systematic expansion beyond the BPS case in Section 3.2.

Expanding (3.7) around $J_\varphi = -2J_\vartheta$ gives a series of the form

$$\vartheta' = \sum_{n=1}^{\infty} \frac{p_n(t, J_\varphi)}{(1 + t^2)^{n+1} (1 + t^2 - J_\varphi t^4)^{n+1/2}} (J_\varphi + 2J_\vartheta)^n, \quad (3.30)$$

with some polynomials p_n and likewise for φ' .

The resulting integrals are all trigonometric functions, which is simply the small k^2 (3.23) expansion of the elliptic integrals. Integrating between $t = 0$ and t_{\max} (3.12), we find

$$\begin{aligned}\phi &= 2 \arctan 2J_\varphi + \frac{1}{J_\varphi^2} \left[-\frac{3 + 8J_\varphi^2}{1 + 4J_\varphi^2} + \frac{3}{2J_\varphi} \arctan 2J_\varphi \right] (J_\varphi + 2J_\vartheta) + \mathcal{O}((J_\varphi + 2J_\vartheta)^2), \\ \theta &= 2 \arctan 2J_\varphi + \frac{1}{J_\varphi^2} \left[-\frac{6 + 20J_\varphi^2}{1 + 4J_\varphi^2} + \frac{3}{J_\varphi} \arctan 2J_\varphi \right] (J_\varphi + 2J_\vartheta) + \mathcal{O}((J_\varphi + 2J_\vartheta)^2).\end{aligned}\quad (3.31)$$

These series can be inverted to give

$$\begin{aligned}J_\varphi &= \frac{\tan(\phi/2)}{2} + \left[\frac{1}{4 \cos^2(\phi/2)} + \frac{\tan^3(\phi/2)}{6(\phi - 2 \tan(\phi/2))} \right] (\phi - \theta) + \mathcal{O}((\phi - \theta)^2), \\ J_\vartheta &= -\frac{\tan(\phi/2)}{4} - \left[\frac{1}{8 \cos^2(\phi/2)} + \frac{\tan^3(\phi/2)}{6(\phi - 2 \tan(\phi/2))} \right] (\phi - \theta) + \mathcal{O}((\phi - \theta)^2).\end{aligned}\quad (3.32)$$

Expanding the action in series also gives trigonometric functions. The lowest order is the BPS case (3.18), and higher-order terms in the $J_\varphi - 2J_\vartheta$ expansion calculate the near-BPS corrections to the potential. As we already proved, no further $\log \epsilon$ terms arise and we only find new power-like divergences, which can be discarded. The potential is then

$$\begin{aligned}U^{(N)}(\phi, \theta) &= \frac{N}{\pi} \left\{ \log \cos \frac{\phi}{2} - \frac{\tan(\phi/2)}{2} (\phi - \theta) - \left[\frac{1}{\cos^2(\phi/2)} + \frac{4 \tan^3(\phi/2)}{3(\phi - 2 \tan(\phi/2))} \right] \frac{(\phi - \theta)^2}{8} \right. \\ &\quad - \frac{\tan(\phi/2)}{\cos^2(\phi/2)} \left[\frac{1}{3} + \frac{2 \tan(\phi/2)}{\phi - 2 \tan(\phi/2)} + \frac{10(13 + \cos \phi) \tan^2(\phi/2)}{27(\phi - 2 \tan(\phi/2))^2} \right. \\ &\quad \left. \left. + \frac{280 \sin^2(\phi/2) \tan^3(\phi/2)}{81(\phi - 2 \tan(\phi/2))^3} \right] (\phi - \theta)^3 + \dots \right\}.\end{aligned}\quad (3.33)$$

3.5 Antiparallel planes limit

The limit $\pi - \phi = \delta \ll 1$ is not much simpler than the general case but is interesting because it calculates the potential between antiparallel planes. It corresponds to taking $J_\varphi \rightarrow \infty$. To retain nonzero θ we should take a double scaling limit $J_\vartheta \rightarrow \infty$ keeping $q = J_\vartheta/J_\varphi^{2/3}$ fixed. The polynomial (3.8) then becomes (with $t = s/J_\varphi^{1/3}$)

$$1 - 4q^2 s^4 - s^6 = -(s^2 - \tau_1)(s^2 - \tau_2)(s^2 - s_{\max}^2). \quad (3.34)$$

To leading order in J_φ , we have

$$\vartheta = -4q \int_0^{s_{\max}} \frac{s \, ds}{\sqrt{1 - 4q^2 s^4 - s^6}} + \mathcal{O}(J_\varphi^{-2/3}). \quad (3.35)$$

Expressing the integral in terms of elliptic integrals (3.22) gives

$$\theta = \frac{8q}{\sqrt{s_{\max}^2 - \tau_1}} \mathbf{F} \left(\arcsin \frac{s_{\max}}{\sqrt{s_{\max}^2 - \tau_2}} \left| \frac{s_{\max}^2 - \tau_2}{s_{\max}^2 - \tau_1} \right. \right) + \mathcal{O}(J_\varphi^{-2/3}). \quad (3.36)$$

This is an implicit relation between q and θ . Similarly for ϕ , expanding (3.7) to leading order in J_φ gives (where all the elliptic integrals have the same arguments as in (3.36))

$$\delta = \pi - \phi = 2J_\varphi^{-1/3} \left[\frac{\tau_1}{\sqrt{s_{\max}^2 - \tau_1}} \mathbf{F} + \sqrt{s_{\max}^2 - \tau_1} \mathbf{E} \right] + \mathcal{O}(J_\varphi^{-1}). \quad (3.37)$$

The action at leading order is

$$S_{\text{M2}} = 4N J_\varphi^{2/3} \left(\frac{\tau_1}{\sqrt{s_{\max}^2 - \tau_1}} \mathbf{F} + \sqrt{s_{\max}^2 - \tau_1} \mathbf{E} \right) + \mathcal{O}(J_\varphi^0). \quad (3.38)$$

Unlike (3.27), here there are no divergences to treat because the $\log \epsilon$ divergence is subleading in J_φ . Using (3.37) to solve for J_φ , we find

$$U^{(N)}(\pi - \delta, \theta) = -\frac{8N}{\pi \delta^2} \left(\frac{\tau_1}{\sqrt{s_{\max}^2 - \tau_1}} \mathbf{F} + \sqrt{s_{\max}^2 - \tau_1} \mathbf{E} \right)^3. \quad (3.39)$$

The dependence on θ is implicit. For small θ , q is small and we can invert (3.36) explicitly

$$\theta = \frac{4\sqrt{\pi}\Gamma(1/3)}{3\Gamma(5/6)} q - \frac{16q^3}{3} + \mathcal{O}(q^5). \quad (3.40)$$

Expanding (3.39) at small q and inverting $q(\theta)$ gives

$$U^{(N)}(\pi - \delta, \theta) = -\frac{8N\sqrt{\pi}\Gamma(2/3)^3}{\Gamma(1/6)^3\delta^2} \left[1 - \frac{3\sqrt{3}}{8\pi}\theta^2 + \left(1 - \frac{3^{5/2}\Gamma(2/3)\Gamma(5/6)^4}{2^{7/3}\pi^3} \right) \frac{9\theta^4}{64\pi^2} + \dots \right] + \frac{2N}{\pi} \log \delta + \dots \quad (3.41)$$

For $\theta = 0$, this matches the original calculation of the antiparallel planes (6.4) [10]. Here we have a perturbative expansion that can easily be continued to higher orders.

The free field result (2.11) is exact in ϕ and θ , but expanding it around $\phi = \pi$ yields

$$U^{(1)}(\pi - \delta, \theta) = \frac{1}{2\pi} \log \sin \delta/2 - \frac{\cos \delta + \cos \theta}{8\pi \sin^2 \delta/2} = -\frac{1 + \cos \theta}{2\pi \delta^2} + \frac{1}{2\pi} \log \delta + \dots \quad (3.42)$$

Like (3.41), this too has a double pole at $\delta = 0$ and a logarithmic correction.

Note the coefficient of the $\log \delta$ term in the holographic expression (3.41) is double that of the $\log \cos \phi/2$ part for the BPS expression in (3.33). That implies that for $\theta = \pi - \delta$, the series above sums up to $\sim \delta^2 \log \delta$, to cancel the power law divergence and fix the prefactor of the log.

4 Lightlike crease

A famous limit of the cusped Wilson loop is when the two rays approach the lightcone in Minkowski space. The resulting anomaly is proportional to the boost parameter between the lines, with a coefficient known as the universal cusp anomalous dimension. It governs hard

processes in QCD [39, 40] and also plays a crucial role in $\mathcal{N} = 4$ SYM, where it is captured by the spinning string solution [41], the cusped Wilson loop in Minkowski space [27], and served as the cornerstone for the analysis of scattering amplitudes in that theory including the BDS ansatz [42] and the Wilson loop scattering amplitude duality [43].

We present here analog calculations for a lightlike crease, starting by the analytic continuation of the solution in Section 3 to imaginary angle ϕ and then writing down solutions in lorentzian AdS including the analogue of the 4-cusp solution, which turns out to be two lightcones joined along a circular lightlike crease.

A different adaptation of the 4-cusp solution to surface operators was studied in [44]. We comment on the differences below.

4.1 Analytic continuation

We first look at the solution in Section 3 and find a limit where ϕ diverges. The equation for φ (3.7) can be integrated over the zeros of the polynomial (3.10) in the denominator, and its integral converges unless the zeros are degenerate. The latter is determined by the vanishing of the discriminant (3.25)

$$J_\varphi^2 = -\frac{2}{27} \left[1 - 36J_\vartheta^2 \pm (1 + 12J_\vartheta^2)^{3/2} \right]. \quad (4.1)$$

We want to get imaginary ϕ , so should take the negative sign and as the result should not depend on θ , we can take $J_\vartheta = 0$ and

$$J_\varphi^2 = -\frac{4}{27}. \quad (4.2)$$

Now we get that φ is given by (3.7)

$$\varphi' = \pm \frac{2it^3}{(t^2 + 3)\sqrt{(1 + t^2)(3 + 4t^2)}}, \quad (4.3)$$

and its integral up to the root $t^2 = -3$ gives $(\pi - \phi)/2$. With a regulator δ , we have

$$\phi = \pi + 4i \int_0^{\sqrt{3i - \delta i}} \frac{t^3 dt}{(t^2 + 3)\sqrt{(1 + t^2)(3 + 4t^2)}}. \quad (4.4)$$

The real part of the integral cancels the factor π , while the imaginary part diverges logarithmically as $\delta \rightarrow 0$. Its coefficient is the residue at $t = \sqrt{3i}$, so we get

$$\phi = -i\sqrt{2} \log |\delta| + \dots \rightarrow i\infty. \quad (4.5)$$

To evaluate the action in that limit, we take the analytic continuation of (3.26). The integral becomes

$$S_{M2} = \frac{4N}{\pi} (-2\pi) \int_\epsilon^{i\sqrt{3} - i\delta} \frac{3^{3/2}(1 + t^2)^{3/2} dt}{t^3(3 + t^2)\sqrt{3 + 4t^2}}. \quad (4.6)$$

Again the pole gives a logarithmic divergence. Taking the residue and comparing against ϕ we find

$$S_{M2} = 8N \frac{\sqrt{2}}{3^{3/2}} \log |\delta| + \dots \rightarrow -\frac{8N|\phi|}{3^{3/2}}, \quad \phi \rightarrow i\infty. \quad (4.7)$$

As in the case of the lightlike cusp [27], we find a result proportional to the boost angle $|\phi|$ and the coefficient may be seen as the analogue of the universal cusp anomalous dimension.

The linear growth of the expectation value at large boost is also present in the free theory. There the analytic continuation is trivial, simply take (2.11) in the limit $\phi \rightarrow i\infty$ to obtain

$$U^{(1)} \rightarrow \frac{|\phi|}{2\pi} + \dots \quad (4.8)$$

We do not know whether there is really a meaning to this expression as a potential and to what extent we should be analytically continuing the solution for the compact crease rather than the infinite one. To address these points we turn now to study the system directly in lorentzian signature.

4.2 Solutions in lorentzian AdS

We now look for solutions to represent the infinite crease in Minkowski space. We use the metric of lorentzian AdS_4 subspace of $AdS_7 \times S^4$

$$ds^2 = \frac{4L^2}{z^2}(dz^2 + (dx^1)^2 + (dx^2)^2 - dt^2) = \frac{4L^2}{z^2}(dz^2 + (dx^1)^2 + d\xi^2 - \xi^2 d\chi^2). \quad (4.9)$$

As world-volume coordinates we take (for $|x^2| > |t|$) $\xi = \sqrt{(x^2)^2 - t^2}$, $\chi = \operatorname{arccoth}(x^2/t)$ and v and the ansatz

$$z = u(\chi)\xi, \quad x^1 = \sqrt{1 + u(\chi)^2}v. \quad (4.10)$$

The scaling of z with ξ is natural because of dilatation invariance of the crease. The scaling of x^1 with $\sqrt{1 + u^2}$ may seem unnatural at first, but it is required to have a full 1d conformal symmetry $SO(2, 1)$ as is discussed in Appendix A. This seems to be one difference from the solution in [44] and there should be more solutions interpolating between the two.

Given this, the lagrangian is

$$\mathcal{L} = 8T_{M2}L^3 \frac{\sqrt{(1 + u^2)(1 + u^2 - u'^2)}}{\xi^2 u^3}. \quad (4.11)$$

Ignoring $8L^3/\xi^2$, the conserved energy is

$$E = \frac{(1 + u^2)^{3/2}}{u^3 \sqrt{1 + u^2 - u'^2}}. \quad (4.12)$$

Inverting this gives

$$\chi = \int \frac{Eu^3 du}{\sqrt{(1 + u^2)(E^2 u^6 - (1 + u^2)^2)}}. \quad (4.13)$$

In these coordinates we can find the solutions that are the analytic continuation of those in Appendix A for finite boost angle. The solutions we get do not cover the entire world volume and they require continuation to $|x^2| \leq |t|$, where we take instead the metric

$$ds^2 = \frac{4L^2}{z^2}(dz^2 + (dx^1)^2 - d\xi^2 + \xi^2 d\chi^2), \quad (4.14)$$

where now $\xi = \sqrt{t^2 - (x^2)^2}$ and $\chi = \operatorname{arccoth}(t/x^2)$.

To study solutions in this patch (4.14), the ansatz is

$$z = u(\chi)\xi, \quad x^1 = \sqrt{u(\chi)^2 - 1}v, \quad (4.15)$$

and the lagrangian becomes

$$\mathcal{L} = 8T_{\text{M2}}L^3 \frac{\sqrt{(u^2 - 1)(u^2 - 1 - u'^2)}}{\xi^2 u^3}. \quad (4.16)$$

The simplest solution to the equations of motion has constant u , where imposing that in the Euler-Lagrange equation for (4.16) gives the relation $u^2 = 3$. In the original coordinate patch this is $u = \pm i\sqrt{3}$, which also arises near the singularity of (4.4), where the solution becomes stationary.

For this solution in the new patch, the action becomes

$$S_{\text{M2}} = \frac{4N}{3\sqrt{3}\pi} \int \frac{dv d\xi d\chi}{\xi^2}. \quad (4.17)$$

This is proportional to the area of AdS_2 times the extent of the coordinate χ . Comparing to (4.7), we see that they agree, if we replace the v, ξ integral with the integral over global euclidean AdS_2 with regularised area -2π .

4.3 Global solutions

The lightlike crease solution above is obtained in the Poincaré patch and can be embedded in global AdS . For the lightlike cusp solution of [27], the analysis of the global structure of the solution revealed that the lightlike cusp is in fact related by a conformal transformation to the lightlike Wilson loop with 4-cusps [28]. Here we find that the single lightlike crease is conformally related to a surface consisting of two lightcones glued along a crease.

Following [27, 28], we can embed our solution into global AdS by writing it in terms of the embedding coordinates

$$\begin{aligned} X_{-1} &= \frac{1}{2z}(L^2 + z^2 - t^2 + (x^i)^2), & X_0 &= \frac{Lt}{z}, \\ X_6 &= -\frac{1}{2z}(-L^2 + z^2 - t^2 + (x^i)^2), & X_i &= \frac{Lx^i}{z}, \end{aligned} \quad (4.18)$$

as

$$X_0^2 - X_2^2 = \frac{L^2}{3}, \quad X_3 = X_4 = X_5 = 0, \quad (4.19)$$

and then $X_{-1}^2 - X_1^2 - X_6^2 = 2L^2/3$. This can be written homogenously as

$$X_{-1}^2 - X_1^2 - X_6^2 = 2X_0^2 - 2X_2^2, \quad X_3 = X_4 = X_5 = 0. \quad (4.20)$$

Conformal transformations are given by rotations of the embedding coordinates, and we can now consider the rotated solution

$$X_0^2 - X_1^2 - X_2^2 = 2X_{-1}^2 - 2X_6^2, \quad X_3 = X_4 = X_5 = 0. \quad (4.21)$$

In the new Poincaré patch, this new solution is

$$z = \sqrt{\frac{3}{2}(t^2 - r^2)}, \quad (4.22)$$

with $r = \sqrt{(x^1)^2 + (x^2)^2}$. For $z = 0$, this is a two-dimensional lightcone $t = r$.

We can write its action as

$$S_{\text{M2}} = \frac{4N}{3\pi} \sqrt{\frac{2}{3}} \int \frac{\sinh \rho}{z} dz d\rho dv, \quad (4.23)$$

where $\rho = \text{arccoth}(t/r)$ and v the angle in the (x^1, x^2) plane parametrising an AdS_2 at fixed z . The integral over AdS_2 is regularised to -2π and the integral over z diverges as $\log z$. This agrees with the analytic continuation (4.7) if we identify the $\log z$ divergence with $|\phi|/\sqrt{2}$.

To obtain a compact surface, we start again with (4.21), swap X_6 with X_3 and map $X_0 \rightarrow (X_0 + X_{-1})/\sqrt{2}$ and $X_{-1} \rightarrow (X_{-1} - X_0)/\sqrt{2}$. We find

$$2X_{-1}^2 - X_0^2 \rightarrow \frac{X_{-1}^2 + X_0^2 - 6X_{-1}X_0}{2} = 2X_3^2 - X_1^2 - X_2^2, \quad X_4 = X_5 = X_6 = 0. \quad (4.24)$$

This can be recast as

$$\frac{z^2}{3} = \frac{1}{2}(t - L)^2 - (x^3)^2, \quad r^2 = 4L^2 + 2(x^3)^2 - \frac{1}{2}(t - 3L)^2. \quad (4.25)$$

Setting $z = 0$ gives the surface on the boundary parametrised by t (and angle v) with two branches

$$x^3 = \pm \frac{L - t}{\sqrt{2}}, \quad r = \frac{L + t}{\sqrt{2}}. \quad (4.26)$$

The physical domain is $-L < t < L$, so $r, |x^3| < \sqrt{2}L$. Each branch parametrises a lightcone emanating from $t = -L$ and $x^3 = \pm\sqrt{2}L$ and merging along a crease at $t = L$, $x^3 = 0$ and $r = \sqrt{2}L$.

It's convenient to parametrise the solution by z , x_3 and v , such that the action is

$$S_{\text{M2}} = \frac{4LN}{\sqrt{3}\pi} \int \frac{dz dx_3 dv}{z^2 \sqrt{z^2 + 3x_3^2}}. \quad (4.27)$$

There are two sources of divergence. First when z goes to 0, which is the usual divergence from the volume of AdS , and then in addition when also $x_3 \rightarrow 0$, which is associated with the crease singularity. Introducing a cutoff $z > \epsilon$ regularises both. To perform the integral, notice that the M2-brane closes in AdS when $r = 0$, which sets the range of x_3 and z to be

$$x_3^2 < \frac{(z - 2\sqrt{3}L)^2 - 6L^2}{3}, \quad z < \sqrt{6}(\sqrt{2} - 1)L. \quad (4.28)$$

Integrating we find

$$S_{\text{M2}} = -\frac{16N}{3} \frac{L}{\epsilon} \log \epsilon + \text{finite}. \quad (4.29)$$

This result is peculiar and is in contradiction to our assertion in Section 2.2 that creases do not suffer from $\epsilon^{-1} \log \epsilon$ divergences. It deserves further exploration.

An alternative regularisation which preserves the AdS_2 symmetry is to write the lorentzian AdS_7 as a foliation over $AdS_2 \times dS_4$, as in the case of the compact crease in Section 3.1. This is the analytic continuation in ν of (3.1). Keeping only the timelike coordinate from the de Sitter component, the metric is

$$ds^2 = L^2 \left[d\nu^2 + \cos^2 \nu (d\rho^2 + \sinh^2 \rho dv^2) - \sin^2 \nu d\varphi^2 \right]. \quad (4.30)$$

The boundary of space is at $\varphi \rightarrow \pm\infty$ or $\rho \rightarrow \infty$. Taking $\nu(\alpha)$ the action is

$$\mathcal{L} = 8T_{M2}L^3 \cosh \rho \cos^2 \nu \sqrt{\sin^2 \nu - \nu'^2}. \quad (4.31)$$

Looking for constant ν solutions gives $\sin^2 \nu = 1/3$ and regularising the AdS_2 area leads to the action

$$S_{M2} = -\frac{8N}{3\sqrt{3}} \int d\varphi, \quad (4.32)$$

which again agrees with the analytic continuation of the potential (4.7) and the action of the lightlike crease (4.17).

5 Defect CFT

As the crease preserves part of the conformal group, it is natural to study it from a defect CFT perspective [45–50]. In particular, we use these techniques to find expressions for the potential as an expansion around BPS configurations, including quadratic order around the plane, producing (1.14) and linear order around the $\theta = \phi$ cusp, resulting in (1.15). This approach does not rely on a particular realisation of the $\mathcal{N} = (2, 0)$ theory and the surface operators, so is applicable to theories with any ADE algebra and surface operators in any representation of the algebra.

The principle at action is very similar to that of the bremsstrahlung function $B(\lambda)$ and “generalised bremsstrahlung function” $B(\phi, \lambda)$ for cusped Wilson loops in $\mathcal{N} = 4$ SYM (with multiple generalisations) [13, 16, 51, 52].

A superconformally invariant surface has a distinguished set of operators restricted to the defect, known as the displacement operator multiplet, with conformal primaries: \mathbb{D}^m ($m = 3, \dots, 6$) for broken translations, \mathbb{O}^i ($i = 2, \dots, 5$) for broken R-symmetries and \mathbb{Q} for broken supercharges [53–56, 6]. For the spherical surface operator, they can be expressed as contact terms for the conservation equations for the energy momentum tensor $T^{\mu\nu}$ and R-current $j^{\mu IJ}$ as

$$\partial_\mu T^{\mu\nu}(x_\parallel, x_\perp) V_{S^2} = e_n^\nu V_{S^2} [\mathbb{D}^n(x_\parallel)] \delta^{(4)}(x_\perp), \quad (5.1)$$

$$\partial_\mu j^{\mu i 1}(x_\parallel, x_\perp) V_{S^2} = V_{S^2} [\mathbb{O}^i(x_\parallel)] \delta^{(4)}(x_\perp). \quad (5.2)$$

There is also a similar equation for broken supersymmetries \mathbb{Q} . Here x_\parallel are the coordinates along the surface and x_\perp are normal. Furthermore, we use the notation $V[\mathbb{D}]$ to denote the insertion of the operator \mathbb{D} on the defect. e_n^ν are the vielbein restricted to the normal space at the point x_\parallel .

These operators are special because, as we review below, their correlators capture the expectation value of small deformations of the conformal defect. We start with the case of deformations of the sphere to find (1.14), and then proceed to study the deformations away from the BPS crease at finite $\phi = \theta$ to derive (1.15).

5.1 Near sphere expansion

Consider a surface which is a small deformation of a sphere. This can be obtained by a local deformation along a normal vector $\xi_\nu(x_\parallel)$. It can be expressed as a six dimensional integral over the derivative of the current $\partial_\mu T^{\mu\nu}$, and including also a local R-symmetry deformation ω^i leads to a formal expression defining the operator $V_{\xi,\omega}$

$$V_{\xi,\omega} = \exp \left[\int d^6x \left(\xi_\nu \partial_\mu T^{\mu\nu} + \omega^i \partial_\mu j^{\mu 1i} \right) \right] V_{S^2}. \quad (5.3)$$

Clearly if ξ and ω are constants, the exponential simply expresses a global translation/R-symmetry rotation. As we allow ξ , ω to vary along the sphere, it describes a local deformations that can affect the expectation value. We adopt spherical coordinates for \mathbb{R}^6

$$ds^2 = dr^2 + r^2 \left(du^2 + \cos^2 u dv^2 + \sin^2 u \left(d\theta_3^2 + \cos^2 \theta_3 \left(d\theta_2^2 + \cos^2 \theta_2 d\theta_1^2 \right) \right) \right), \quad (5.4)$$

and the sphere is located at $\theta_{1,2,3} = 0$, $r = R$. ξ , ω are now functions of u , v , and since ξ is a normal vector, it can have components ∂_{θ_1} , ∂_{θ_2} , ∂_{θ_3} and ∂_r .

We can calculate the expectation value of $V_{\xi,\omega}$ for small ξ , ω by expanding the exponential in (5.3). At the linear order, using (5.2), we get insertions of displacement operators into the surface operator

$$R^2 \int \cos u du dv \left(\xi_\nu(u, v) e'_n V_{S^2}[\mathbb{D}^n(u, v)] + \omega^i(u, v) V_{S^2}[\mathbb{O}^i(u, v)] \right). \quad (5.5)$$

The factor $R^2 \cos u$ comes from the metric on the sphere of radius R .

These terms do not contribute to the expectation value since 1-point functions vanish by symmetry. The first nontrivial contribution is instead at quadratic order, where we find pairs of displacement operators from the currents acting on V . In addition there are contact terms from the currents acting on defect operators. This can be seen as delta function contributions to the $\mathbb{D}\mathbb{D}$ and $\mathbb{O}\mathbb{O}$ OPEs, giving

$$\begin{aligned} \partial_\mu j^{\mu 1i}(u, v, x^\perp) V_{S^2}[\mathbb{O}^j(u', v')] &= V_{S^2}[\mathbb{O}^i(u, v) \mathbb{O}^j(u', v')] \delta^{(4)}(x^\perp) \\ &+ \frac{\alpha}{R^2} V_{S^2}[\mathbb{1}] \delta^{ij} \delta^{(4)}(x^\perp) \delta(\sin(u - u')) \delta(v - v'), \end{aligned} \quad (5.6)$$

$$\begin{aligned} \partial_\mu T^{\mu\nu}(u, v, x^\perp) V_{S^2}[\mathbb{D}^n(u', v')] &= V_{S^2}[e'_m \mathbb{D}^m(u, v) \mathbb{D}^n(u', v')] \delta^{(4)}(x^\perp) \\ &+ \frac{\beta}{R^4} V_{S^2}[\mathbb{1}] e'_m \delta^{mn} \delta^{(4)}(x^\perp) \delta(\sin(u - u')) \delta(v - v'). \end{aligned} \quad (5.7)$$

The contact terms come with unknown prefactors α and β and only the identity part of the singular OPE is retained, since all other 1-point functions vanish. These terms come with appropriate powers of R , on dimensional grounds, so they don't appear in the dCFT description of the plane in [6].

Using (5.6), (5.7) we obtain the change in expectation value for arbitrary $\xi(u, v)$, $\omega(u, v)$

$$\begin{aligned} \langle V_{\xi, \omega} \rangle - \langle V_{S^2} \rangle &= \frac{R^4}{2} \int \cos u \, du \, dv \cos u' \, du' \, dv' \, \omega^i \omega^j \langle V_{S^2} [\mathbb{O}^i(u, v) \mathbb{O}^j(u', v')] \rangle \\ &+ \frac{R^4}{2} \int \cos u \, du \, dv \cos u' \, du' \, dv' \, \xi^\mu e_\mu^m \xi^\nu e_\nu^n \langle V_{S^2} [\mathbb{D}^m(u, v) \mathbb{D}^n(u', v')] \rangle \quad (5.8) \\ &+ \frac{1}{2} \langle V_{S^2} \rangle \int \left(\alpha \omega^2 + \frac{\beta \xi^2}{R^2} \right) \cos u \, du \, dv + \dots \end{aligned}$$

The 2-point functions of \mathbb{D} and \mathbb{O} that enter this expression are fixed by their dimensions 3 and 2 respectively and for the spherical surface are

$$\frac{\langle V_{S^2} [\mathbb{D}^m(u, v) \mathbb{D}^n(u', v')] \rangle}{\langle V_{S^2} \rangle} = \frac{C_{\mathbb{D}}}{8\pi^2 R^6} \frac{\delta^{mn}}{(1 - \sin u \sin u' - \cos u \cos u' \cos(v - v'))^3}, \quad (5.9)$$

$$\frac{\langle V_{S^2} [\mathbb{O}^i(u, v) \mathbb{O}^j(u', v')] \rangle}{\langle V_{S^2} \rangle} = \frac{C_{\mathbb{O}}}{4\pi^2 R^4} \frac{\delta^{ij}}{(1 - \sin u \sin u' - \cos u \cos u' \cos(v - v'))^2}. \quad (5.10)$$

The normalisation of \mathbb{D} is fixed by (5.2), so $C_{\mathbb{D}}$ and $C_{\mathbb{O}}$ on the right hand side are not arbitrary and are part of the dCFT data. In fact, for any surface operator in a CFT, it was shown in [57] that $C_{\mathbb{D}}$ is related to the coefficient a_2 entering the conformal anomaly (1.8) as $C_{\mathbb{D}} = -16a_2$. For the $\mathcal{N} = (2, 0)$ theory, supersymmetry implies that $a_2 = -c$ and the normalisation of the 2-point function of \mathbb{O} is given by $C_{\mathbb{O}} = c$ [6].

It is now a simple matter to fix α and β . Taking ξ to be any conformal Killing vector, for example ∂_{θ_1} , leads to a global rotation which should not change the expectation value. This fixes the constant β . We can also fix α by taking $\omega^i = \delta^{i2}$ to generate a constant R-symmetry rotation. Performing the integrals (5.8) with these values of ξ , ω , we find

$$\alpha = \frac{c}{4\pi}, \quad \beta = -\frac{3c}{2\pi}. \quad (5.11)$$

With α , β in hand, we now evaluate (5.8) for the case of the crease of angle ϕ , θ as defined in (1.4) and (1.3). We take

$$\omega^i = \begin{cases} \theta \delta^{i2}, & u > 0 \\ 0, & u < 0 \end{cases}, \quad \xi^\mu e_\mu^m = \begin{cases} \phi e_{\theta_1}^m = \phi R \sin u \delta^{6m}, & u > 0 \\ 0, & u < 0 \end{cases}, \quad (5.12)$$

which rotates one of the hemisphere by an angle ϕ and the scalar coupling by θ . Plugging these in (5.8) and performing the integrals we obtain

$$\frac{\langle V_{\phi, \theta} \rangle}{\langle V_{S^2} \rangle} = 1 + \frac{c}{4} (\theta^2 - 2\phi^2) + \dots \quad (5.13)$$

from which (1.14) follows directly. This is also in agreement with the expansion of the explicit results (2.11) and (3.19).

5.2 Near-BPS expansion

The previous subsection relied on the defect CFT description of the deformation of the sphere. To study the crease with finite angles ϕ , θ , we now turn to the formulation of the defect CFT description of deformations of the crease itself.

It is easiest to derive the formalism for the infinite crease and then use a conformal transformation to apply it to the spherical crease. The symmetries of the infinite crease (1.2) are $\mathfrak{so}(2, 1) \oplus \mathfrak{so}(3) \oplus \mathfrak{so}(3)$, corresponding respectively to the 1d conformal group acting on both half-planes, transverse rotations in $x^{4,5,6}$ and transverse R-symmetry rotations of $n^{3,4,5}$. Note that from the point of view of symmetries, this setup is identical to inserting a line operator inside the plane. According to the classification of [58], this is a supersymmetric line defect breaking the transverse rotational symmetry.

On the sphere or plane, \mathbb{D}^m and \mathbb{O}^i are quartets of a pair of $\mathfrak{so}(4)$ symmetries, broken to $\mathfrak{so}(3)$ by the crease. This singles out one displacement \mathbb{D}^3 (for the crease in the (2, 3) plane extended in the x^1 direction) and one R-rotation \mathbb{O}^2 that are singlets and can therefore have expectation values. Another way to say this is that these operators are no longer primaries and they mix with the identity. Explicitly we have

$$\langle V_{\phi,\phi}[\mathbb{D}^3(x_2)] \rangle = \frac{h_{\mathbb{D}}(\phi)}{x_2^3}, \quad (5.14)$$

with the power in the denominator fixed by the conformal dimension of \mathbb{D} and $h_{\mathbb{D}}$ is an unknown constant. Likewise,

$$\langle V_{\phi,\phi}[\mathbb{O}^2(x_2)] \rangle = \frac{h_{\mathbb{O}}(\phi)}{x_2^2}. \quad (5.15)$$

In addition to these bosonic symmetries, when $\phi = \theta$ the crease preserves 4Q's which offer more relations. Using γ for the 6d gamma matrices and ρ for the R-symmetry matrices (see [7] for notations), the unbroken supersymmetries are those satisfying

$$(1 + i\rho_1\gamma_{12})\mathbb{Q}_+ = (1 + i\rho_2\gamma_{13})\mathbb{Q}_+ = 0. \quad (5.16)$$

These are 2 independent constraints, so they select 4 out of the 16 supersymmetries of the $\mathcal{N} = (2, 0)$ theory. Similarly, there are also 4 preserved S conformal supercharges. Note that in this equation and below we suppress the spinor indices.

Along with the bosonic part, the symmetries assemble into $\mathfrak{osp}(4^*|2)$ and impose further constraints on the correlators (5.14) and (5.15) relating $h_{\mathbb{D}}$ and $h_{\mathbb{O}}$. To derive them, consider acting with one of the supersymmetry \mathbb{Q}_+ on the one-point function

$$\langle \mathbb{Q}_+ V_{\phi,\phi}[\mathbb{Q}] \rangle = 0. \quad (5.17)$$

Away from $x_2 = 0$, the transformations under supersymmetry of \mathbb{Q} are the same as on the plane, which were obtained in [6]. They read (with $a = 1, 2$)

$$\begin{aligned} \mathbb{Q}\mathbb{D}_m &= \frac{1}{2}\gamma_{am}\partial^a\mathbb{Q}, \\ \mathbb{Q}\mathbb{Q} &= 2\gamma_m\mathbb{D}^m + 2\rho_{1i}\gamma_a\partial^a\mathbb{O}^i, \\ \mathbb{Q}\mathbb{O}_i &= \frac{1}{2}\rho_{1i}\mathbb{Q}, \end{aligned} \quad (5.18)$$

for any of the supersymmetries \mathbb{Q} preserved by the plane. Restricting these transformations to the subset \mathbb{Q}_+ also preserved by the crease, we can evaluate (5.17) to find

$$\langle \mathbb{Q}_+ V_{\phi,\phi}[\mathbb{Q}] \rangle = 2 \left[\gamma_3 \langle V_{\phi,\phi}[\mathbb{D}^3] \rangle - \gamma_{23}\gamma_a\partial^a \langle V_{\phi,\phi}[\mathbb{O}^2] \rangle \right] = 0. \quad (5.19)$$

To obtain this, we used (5.16) to eliminate ρ in favor of γ matrices. Clearly the derivative is only nonzero along x_2 . We are left with

$$\langle V_{\phi,\phi}[\mathbb{D}^3(x_2)] \rangle = -\partial_2 \langle V_{\phi,\phi}[\mathbb{O}^2(x_2)] \rangle \quad \Leftrightarrow \quad h_{\mathbb{D}}(\phi) = 2h_{\mathbb{O}}(\phi). \quad (5.20)$$

We can now use this constraint to study small deformations of the spherical crease. A conformal transformation of the above relations now gives

$$\frac{\langle V_{\phi,\phi}[\mathbb{D}^3(u,v)] \rangle}{\langle V_{\phi,\phi} \rangle} = \frac{h_{\mathbb{D}}(\phi)}{R^3 \sin^3 u}, \quad \frac{\langle V_{\phi,\phi}[\mathbb{O}^2(u,v)] \rangle}{\langle V_{\phi,\phi} \rangle} = \frac{h_{\mathbb{O}}(\phi)}{R^2 \sin^2 u}. \quad (5.21)$$

Following the same logic as in Section 5.1, we can relate the constants $h_{\mathbb{D}}$ and $h_{\mathbb{O}}$ to derivatives of the potential. For instance, integrating the one-point function of \mathbb{O}^2 calculates the small angle expansion around the BPS case

$$\langle V_{\phi,\theta} \rangle = \langle V_{\phi,\phi} \rangle - R^2(\theta - \phi) \int_0^{\pi/2} \cos u \, du \int_0^{2\pi} dv \langle V_{\phi,\phi}[\mathbb{O}^2(u)] \rangle + \dots \quad (5.22)$$

Plugging (5.21) and integrating we find

$$\frac{1}{\pi} \frac{d}{d\theta} \exp(2\pi U(\phi, \theta)) \Big|_{\theta=\phi} = -2h_{\mathbb{O}}(\phi) \int_0^{\pi/2} \frac{\cos u \, du}{\sin^2 u} \int_0^{2\pi} dv. \quad (5.23)$$

The right-hand side contains the integral over AdS_2 in the disc topology. After regularisation this integrates to -2π . We then obtain

$$h_{\mathbb{O}}(\phi) = \frac{1}{4\pi^2} \frac{d}{d\theta} \exp(2\pi U(\phi, \theta)) \Big|_{\theta=\phi}. \quad (5.24)$$

In a similar way $h_{\mathbb{D}}$ is related to the derivative with respect to ϕ . Integrating the one-point function gives

$$\langle V_{\phi,\theta} \rangle = \langle V_{\theta,\theta} \rangle + R^2(\phi - \theta) \int_0^{\pi/2} \cos u \, du \int_0^{2\pi} dv e^3_{\theta_1} \langle V_{\phi}[\mathbb{D}^3(u)] \rangle + \dots \quad (5.25)$$

Again the integral gives the volume of AdS_2 and leads to

$$h_{\mathbb{D}}(\phi) = -\frac{1}{4\pi^2} \frac{d}{d\phi} \exp(2\pi U(\phi, \theta)) \Big|_{\theta=\phi}. \quad (5.26)$$

Finally, comparing (5.24) with (5.26) and using (5.20) we obtain a relation between the first derivatives of the potential

$$\frac{dU(\phi, \theta)}{d\phi} \Big|_{\phi=\theta} = -2 \frac{dU(\phi, \theta)}{d\theta} \Big|_{\theta=\phi}. \quad (5.27)$$

Therefore, expanding the potential in Taylor series, we find

$$\begin{aligned} U(\phi, \theta) &= U(\phi, \phi) + (\theta - \phi) \frac{dU(\phi, \theta)}{d\theta} \Big|_{\theta=\phi} + \dots \\ &= U(\phi, \phi) + (\phi - \theta) \frac{dU(\phi, \phi)}{d\phi} + \dots \end{aligned} \quad (5.28)$$

This proves (1.15).

The explicit expressions in (1.13) with $C = c$ then gives

$$h_{\mathbb{D}} = 2h_{\mathbb{O}} = \frac{c}{2\pi^2} \cos^{2c} \frac{\phi}{2} \tan \frac{\phi}{2} = -\partial_{\phi} \left[\frac{1}{4\pi^2} \cos^{2c} \frac{\phi}{2} \right]. \quad (5.29)$$

It would be interesting to try to derive this relation between $h_{\mathbb{D}}$ and c , which would then prove that the leading form of the potential is indeed (1.13).

6 Conclusion

In this paper we defined and studied several realisations of the crease surface observable in the $\mathcal{N} = (2, 0)$ theory. We were able to define a quantity $U(\phi, \theta)$, which can be thought of as a surface-antisurface potential, and calculated it in the abelian theory and using classical M2-branes in holography.

For $\theta = \phi$ the surfaces preserve at least eight supercharges and the function $U(\phi, \phi)$ takes the simple form (1.12) proportional to $\log \cos(\phi/2)$ in both calculations. Furthermore, the proportionality constant C is equal in both cases to the anomaly coefficient c in (1.9), (1.10), leading us to conjecture that it is true at any N .

It is natural to draw an analogy with cusped Wilson loops in supersymmetric gauge theories and in particular $\mathcal{N} = 4$ SYM. One clear point of deviation are the anomalies—Wilson loop are anomalous only in the presence of a cusp, while surface observables are anomalous also for the spherical geometry. Furthermore, the natural quantity to associate to the cusp is its anomaly which depends on its angle, while the surface anomaly is independent of the angle meaning that the ratio $\langle V_{\phi, \phi} \rangle / \langle V_{S^2} \rangle$ is well-defined and finite.

The comparison is most straightforward then in the BPS case when the cusped Wilson loop is not anomalous, but still can provide a finite expectation value, when taking the two longitude configuration on S^2 (or a compact cusp), for which the expectation value is related to that of the circular Wilson loop $W_{\circ}(N, \lambda)$ [59–62] as

$$\langle W_{\phi, \phi}(N, \lambda) \rangle = \langle W_{0,0}(N, \tilde{\lambda}) \rangle \equiv \langle W_{\circ}(N, \tilde{\lambda}) \rangle, \quad \tilde{\lambda} = \left(1 - \frac{\phi^2}{\pi^2} \right) \lambda, \quad (6.1)$$

and the expectation value of the circular Wilson loop is [23–25]

$$\langle W_{\circ}(N, \lambda) \rangle = \frac{1}{N} L_{N-1}^1 \left(-\frac{\lambda}{4N} \right) e^{\frac{\lambda}{8N}}. \quad (6.2)$$

For the surface operator, we have the potential as calculated from the spherical crease in equation (1.12) $U(\phi, \phi) = \frac{c}{\pi} \log \cos(\phi/2)$ with the proportionality constant c being the anomaly coefficient (1.10).

The BPS Wilson loop depends on three parameters: N , λ and ϕ , but the latter are combined into the effective coupling $\tilde{\lambda}$. Still the resulting expression has a rich interplay of N and $\tilde{\lambda}$, while in the absence of a marginal coupling in the $\mathcal{N} = (2, 0)$ theory, the BPS potential is a factorised function of the integer N and continuous angle ϕ . For surfaces in higher representations, the expression (1.10) gets modified accordingly [20–22], and the same is true for the Wilson loop (6.2) [63–70].

Although we couldn't prove (1.12) for any N , we did prove rigorously that for small ϕ the potential has the form (1.14), with $C = c$, as well as the relation (1.15) for the near-BPS behaviour.

This is also completely analogous to the cusped Wilson loop. While the functions that appear are different, in both cases the near-BPS expansion is given by the derivative with respect to the angle ϕ of the BPS result. For the cusped Wilson loop the generalised bremsstrahlung function [13] can be written as

$$B(\phi, \lambda, N) = -\frac{1}{2} \partial_\phi \log \langle W_{\phi, \phi}(N, \lambda) \rangle, \quad (6.3)$$

and the result for the crease (1.13), (1.15) is identical. This relation for the near BPS expansion is guaranteed by the defect CFT analysis in Section 5.2, based on the residual supersymmetry preserved by the crease. In the presence of the crease, there is a displacement operator \mathbb{D} that develops a 1-point function, and likewise for its superpartner \mathbb{O} . Their expectation value calculates first derivatives of the potential, and the relations between them allows to derive (1.15).

Going beyond the quadratic order around the plane, or beyond linear deviations from the crease requires far more complicated calculations. In the former, it requires the 4-point function of displacements and in the latter the 2-point function of the singlet displacement. The 4-point function of the displacement operator in the Wilson loop is well studied [71–74] and nontrivial relations among them were found in [75, 76]. The same was done for the surface operators in [5, 76], but it certainly deserves further study.

The potential $U(\phi, \theta)$ is well-defined also away from the BPS limit and we calculated it both in the free theory and at large N . Here one would wish to invoke the analogy to the generalised cusp anomalous dimension of [12], with the caveat, that the latter is an anomaly while the divergence in the potential is regularised either to zero in the case of the infinite crease, or to a finite -2π (multiplying U) in the case of the spherical crease.

Regardless of this analogy, $U(\phi, \theta)$ allows to interpolate between the plane and the antiparallel planes (or more properly between the sphere and to coincident hemispheres). For planes separated a distance D and with opposite orientation, it was found in [38] that the potential density is

$$\mathcal{E} = -\frac{8N\sqrt{\pi}\Gamma(2/3)}{\Gamma(1/6)^3} \frac{1}{D^2}. \quad (6.4)$$

The dependence on the distance is fixed by conformal symmetry but the prefactor, which is not, was one of the first predictions of the AdS/CFT correspondence. Among other things, we generalise this expression to include an R-symmetry angle θ between the planes (3.41). We also obtained the explicit M2-brane for any angle and can calculate the potential for arbitrary ϕ and θ , although the dependence on the angles is implicit.

Another natural limit is $\phi \rightarrow i\infty$, for which the potential grows linearly in $|\phi|$ (4.7), with no obvious relation between the prefactors at $N = 1$ and $N \rightarrow \infty$. This limit can be interpreted as calculating the action for the lightlike crease in Minkowski space, which we verify by obtaining the minimal M2-brane in lorentzian AdS and comparing its action to the potential. By embedding the lightlike crease solution in global AdS we also obtain a solution describing two lightcones glued along a crease, which is the analogous to the 4-cusp lightlike Wilson loop of [27, 28]. It would be interesting to see if the lightlike cones and creases have a physical interpretation similar to the lightlike Wilson loops, which calculate scattering amplitudes in $\mathcal{N} = 4$ SYM. The lightlike cusp is also related by an analytic

continuation [77] to the rotating string [41], and it would be interesting to check whether the solutions presented in Section 4 are related to the rotating membrane solutions obtained in [78, 79].

In this paper we found finite, well-defined observables associated to surface operators in the $\mathcal{N} = (2, 0)$ theory, including some BPS protected observables and some that are not. There are many more BPS protected observables found in [7] that merit further study. And many of them may have natural non-BPS extensions. Unraveling them offers a window into the dynamics of this mysterious theory.

To point out just one example, there is a family of 1/4 BPS cones interpolating between the plane and the cylinder. The BPS cylinder which was studied in [8] has a finite nonzero expectation value. The classical M2-brane solutions for the cones of finite angles, whether BPS or not have not been found yet. It should be noted that they are related under dimensional reduction to BPS “latitude” Wilson loops of 5d SYM [17] on S^5 .

Another natural direction is to study creases in surface operators in different theories in varied dimensions.

Acknowledgements

We would like to thank Lorenzo Di Pietro for illuminating discussions, and Arkady Tseytlin, Yifan Wang for their helpful comments on the manuscript. MT gratefully acknowledges support from King’s College London, Université Laval, the Simons Center for Geometry and Physics, Stony Brook University and New York University, where part of this project was realised. His visit to KCL was supported by ERC Consolidator Grant No. 681908, “Quantum black holes: A microscopic window into the microstructure of gravity.” This research was supported in part by Perimeter Institute for Theoretical Physics. Research at Perimeter Institute is supported by the Government of Canada through the Department of Innovation, Science and Economic Development and by the Province of Ontario through the Ministry of Research and Innovation. ND’s research is supported by the Science Technology & Facilities council under the grants ST/T000759/1 and ST/P000258/1.

A Infinite crease in the Poincaré patch

A.1 Solution

Most of the paper is focused on the compact crease and the holographic section (Section 3) used the $AdS_2 \times S^1$ picture. It is interesting to redo the calculation for the infinite crease whose holographic description should be in the Poincaré patch.

As before, we can focus on an $AdS_4 \times S^1$ subspace of $AdS_7 \times S^4$ and now use the metric

$$ds^2 = \frac{y}{L} \left((dx^1)^2 + dr^2 + r^2 d\varphi^2 \right) + \frac{L^2}{y^2} \left(dy^2 + y^2 d\vartheta^2 \right). \quad (\text{A.1})$$

Here r and φ are polar coordinates in the (x^2, x^3) plane, y is the radial coordinate in AdS , and if we change coordinates to $y = 4L^3/z^2$ we get the metric in the form

$$ds^2 = \frac{4L^2}{z^2} (dz^2 + (dx^1)^2 + dr^2 + r^2 d\varphi^2) + L^2 d\vartheta^2. \quad (\text{A.2})$$

As world-volume coordinates we take u, v and r and the ansatz

$$z = ur, \quad x^1 = \sqrt{1+u^2}v, \quad \varphi = \varphi(u), \quad \vartheta = \vartheta(u). \quad (\text{A.3})$$

The scaling of z with r is natural because of dilatation invariance of the crease as in the case of the cusp [11]. The scaling of x^1 with $\sqrt{1+u^2}$ may seem unnatural at first, but it is required to have a full 1d conformal symmetry $SO(2,1)$. To see that we write the induced metric

$$4L^2 \left[\frac{1+u^2}{u^2} \frac{dr^2 + dv^2}{r^2} + \left(r^2 + \frac{u^2 v^2}{1+u^2} + r^2 \varphi'^2 + \frac{r^2 u^2}{4} \vartheta'^2 \right) \frac{du^2}{r^2 u^2} + \frac{2ur du dr + 2uv du dv}{r^2 u^2} \right]. \quad (\text{A.4})$$

Fixed u slices are clearly AdS_2 , and hence the required symmetry.

It is possible to solve the equations of motion also without this extra factor of $\sqrt{1+u^2}$ in x^1 , but the solution does not correspond to the conformally invariant crease that we are studying here.

Comparing to (3.2), we see that we should identify u with t and indeed the resulting lagrangian is then identical to (3.5) with the replacement of the measure factors

$$\sinh \rho d\rho dv \rightarrow \frac{dr dv}{r^2}. \quad (\text{A.5})$$

The equations of motion are then the same, but the total action vanishes because the natural regularisation of the area of AdS_2 in this coordinate system is zero. One can also implement other regularisations, with a cutoff on z instead of r and possibly restrict x^1 to a fixed length, rather than set a cutoff on v . Those calculations yield different (and complicated) expressions.

A.2 Calibration equations

Here we derive the BPS condition (3.9) used in section 3.2 from the calibration equations obtained in [7].

Of the four main families of BPS operators identified in [7], the infinite crease falls into two families, type- \mathbb{R} and type- \mathbb{H} . For each of the families there exists a calibration form ϕ such that the surface satisfies the set of equations

$$\partial_m X^M = \frac{1}{2} g_{ml} \varepsilon^{lnp} G^{ML} \phi_{LNP} \partial_n X^N \partial_p X^P. \quad (\text{A.6})$$

Here X^M are the target space coordinates with metric G_{MN} , m are the world-volume indices with induced metric g_{mn} and ε_{mnp} is the Levi-Civita tensor density.

Using the metric

$$ds^2 = \frac{y}{L} dx^\mu dx^\mu + \frac{L^2}{y^2} dy^I dy^I, \quad (\text{A.7})$$

with $\mu = 1, \dots, 6$, $I = 1, \dots, 5$ and $y = |y|$, all surfaces of type \mathbb{R} are calibrated with respect to the form

$$\phi^{\mathbb{R}} = -dx^1 \wedge \sum_{I=1}^5 (dx^{I+1} \wedge dy^I). \quad (\text{A.8})$$

For the coordinates relevant for the infinite crease (A.1), this reduces to

$$\phi^{\mathbb{R}} \Big|_{AdS_3 \times S^1} = -dx^1 \wedge [\cos(\varphi - \vartheta)(dr \wedge dy + ry d\varphi \wedge d\vartheta) + \sin(\varphi - \vartheta)(y dr \wedge d\vartheta + r dy \wedge d\varphi)]. \quad (\text{A.9})$$

Surfaces of type \mathbb{H} have the calibration form

$$\phi^{\mathbb{H}} = \frac{1}{2}\eta_{\mu\nu}^I dx^\mu \wedge dx^\nu \wedge dy^I - \frac{L^3}{y^3} dy_1 \wedge dy_2 \wedge dy_3, \quad (\text{A.10})$$

with $\eta_{\mu\nu}^I$ the 't Hooft symbol in 4d

$$\eta_{12}^3 = \eta_{34}^3 = \eta_{31}^2 = \eta_{24}^2 = \eta_{14}^1 = \eta_{23}^1 = 1. \quad (\text{A.11})$$

This form is supported on $AdS_5 \times S^2$. The crease solution is in $AdS_3 \times S^1$, but it is useful to keep $AdS_3 \times S^2$ components. For the orientation of the crease along x^1 we should replace $y^1 \rightarrow y^3, y^3 \rightarrow -y^1$ in the above, and then the calibration form is

$$\begin{aligned} \phi^{\mathbb{H}}|_{AdS_3 \times S^2} &= \phi^{\mathbb{R}}|_{AdS_3 \times S^1} + dy^3 \wedge \left(dx^2 \wedge dx^3 - \frac{L^3}{y^3} dy^1 \wedge dy^2 \right) \\ &= \phi^{\mathbb{R}}|_{AdS_3 \times S^1} + dy^3 \wedge \left(r dr \wedge d\varphi - \frac{L^3}{y^2} dy \wedge d\vartheta \right). \end{aligned} \quad (\text{A.12})$$

The extra structure in $\phi^{\mathbb{H}}$ is useful because y^3 vanishes identically, so taking $X^M = y^3$ in (A.6) we find

$$\varepsilon^{lnp} \phi_{y^3 NP} \partial_n X^N \partial_p X^P = 0, \quad (\text{A.13})$$

and in particular with the derivatives with respect to r and u (the latter written as prime) this is

$$r\varphi' - \frac{L^3}{y^2} \partial_r(y)\vartheta' = r \left(\varphi' + \frac{u^2}{2} \vartheta' \right) = 0. \quad (\text{A.14})$$

This reproduces the BPS condition (3.9) and therefore shows that the solution with $J_\vartheta = -2J_\varphi$ is indeed BPS. Note that the other components of (A.6) also imply the rest of the equations of motion (3.7).

References

- [1] A. Sen, “Self-dual forms: Action, Hamiltonian and compactification,” *J. Phys. A* **53** no. 8, (2020) 084002, [arXiv:1903.12196](#).
- [2] N. Lambert, A. Lipstein, R. Mouland, and P. Richmond, “Five-dimensional non-Lorentzian conformal field theories and their relation to six-dimensions,” *JHEP* **03** (2021) 053, [arXiv:2012.00626](#).
- [3] L. Mezincescu and P. K. Townsend, “On chiral bosons in 2D and 6D,” [arXiv:2204.09336](#).
- [4] N. Drukker, M. Probst, and M. Trépanier, “Surface operators in the 6d $\mathcal{N} = (2, 0)$ theory,” *J. Phys. A* **53** no. 36, (2020) 365401, [arXiv:2003.12372](#).
- [5] N. Drukker, S. Giombi, A. A. Tseytlin, and X. Zhou, “Defect CFT in the 6d (2, 0) theory from M2 brane dynamics in $AdS_7 \times S^4$,” *JHEP* **07** (2020) 101, [arXiv:2004.04562](#).
- [6] N. Drukker, M. Probst, and M. Trépanier, “Defect CFT techniques in the 6d $\mathcal{N} = (2, 0)$ theory,” *JHEP* **03** (2021) 261, [arXiv:2009.10732](#).

- [7] N. Drukker and M. Trépanier, “Observations on BPS observables in 6d,” *J. Phys. A* **54** no. 20, (2021) 20, [arXiv:2012.11087](#).
- [8] N. Drukker and M. Trépanier, “M2-doughnuts,” *JHEP* **02** (2022) 071, [arXiv:2111.09385](#).
- [9] D. E. Berenstein, R. Corrado, W. Fischler, and J. M. Maldacena, “The operator product expansion for Wilson loops and surfaces in the large N limit,” *Phys. Rev.* **D59** (1999) 105023, [hep-th/9809188](#).
- [10] J. M. Maldacena, “Wilson loops in large N field theories,” *Phys. Rev. Lett.* **80** (1998) 4859–4862, [hep-th/9803002](#).
- [11] N. Drukker, D. J. Gross, and H. Ooguri, “Wilson loops and minimal surfaces,” *Phys. Rev.* **D60** (1999) 125006, [hep-th/9904191](#).
- [12] N. Drukker and V. Forini, “Generalized quark-antiquark potential at weak and strong coupling,” *JHEP* **06** (2011) 131, [arXiv:1105.5144](#).
- [13] D. Correa, J. Henn, J. Maldacena, and A. Sever, “An exact formula for the radiation of a moving quark in $\mathcal{N} = 4$ super Yang Mills,” *JHEP* **06** (2012) 48, [arXiv:1202.4455](#).
- [14] N. Drukker, “Integrable Wilson loops,” *JHEP* **10** (2013) 135, [arXiv:1203.1617](#).
- [15] D. Correa, J. Maldacena, and A. Sever, “The quark anti-quark potential and the cusp anomalous dimension from a TBA equation,” *JHEP* **08** (2012) 134, [arXiv:1203.1913](#).
- [16] N. Gromov and A. Sever, “Analytic solution of bremsstrahlung TBA,” *JHEP* **11** (2012) 075, [arXiv:1207.5489](#).
- [17] M. Mezei, S. S. Pufu, and Y. Wang, “Chern-Simons theory from M5-branes and calibrated M2-branes,” *JHEP* **08** (2019) 165, [arXiv:1812.07572](#).
- [18] A. Schwimmer and S. Theisen, “Entanglement entropy, trace anomalies and holography,” *Nucl. Phys.* **B801** (2008) 1–24, [arXiv:0802.1017](#).
- [19] C. R. Graham and E. Witten, “Conformal anomaly of submanifold observables in AdS/CFT correspondence,” *Nucl. Phys.* **B546** (1999) 52–64, [hep-th/9901021](#).
- [20] J. Estes, D. Krym, A. O’Bannon, B. Robinson, and R. Rodgers, “Wilson surface central charge from holographic entanglement entropy,” *JHEP* **05** (2019) 032, [arXiv:1812.00923](#).
- [21] A. Chalabi, A. O’Bannon, B. Robinson, and J. Sisti, “Central charges of 2d superconformal defects,” *JHEP* **05** (2020) 095, [arXiv:2003.02857](#).
- [22] Y. Wang, “Surface defect, anomalies and b-extremization,” *JHEP* **11** (2021) 122, [arXiv:2012.06574](#).
- [23] J. K. Erickson, G. W. Semenoff, and K. Zarembo, “Wilson loops in $\mathcal{N} = 4$ supersymmetric Yang-Mills theory,” *Nucl. Phys.* **B582** (2000) 155–175, [hep-th/0003055](#).
- [24] N. Drukker and D. J. Gross, “An exact prediction of $\mathcal{N} = 4$ SUSYM theory for string theory,” *J. Math. Phys.* **42** (2001) 2896–2914, [hep-th/0010274](#).
- [25] V. Pestun, “Localization of gauge theory on a four-sphere and supersymmetric Wilson loops,” *Commun. Math. Phys.* **313** (2012) 71–129, [arXiv:0712.2824](#).
- [26] B. Fiol, B. Garolera, and A. Lewkowycz, “Exact results for static and radiative fields of a quark in $\mathcal{N} = 4$ super Yang-Mills,” *JHEP* **05** (2012) 093, [arXiv:1202.5292](#).
- [27] M. Kruczenski, “A Note on twist two operators in $\mathcal{N} = 4$ SYM and Wilson loops in Minkowski signature,” *JHEP* **12** (2002) 024, [hep-th/0210115](#).

- [28] L. F. Alday and J. M. Maldacena, “Gluon scattering amplitudes at strong coupling,” *JHEP* **06** (2007) 064, [arXiv:0705.0303](#).
- [29] E. Witten, “Five-branes and M-theory on an orbifold,” *Nucl. Phys. B* **463** (1996) 383–397, [hep-th/9512219](#).
- [30] D. M. Kaplan and J. Michelson, “Zero modes for the $D = 11$ membrane and five-brane,” *Phys. Rev. D* **53** (1996) 3474–3476, [hep-th/9510053](#).
- [31] A. Gustavsson, “Conformal anomaly of Wilson surface observables: A field theoretical computation,” *JHEP* **07** (2004) 74, [hep-th/0404150](#).
- [32] M. Henningson and K. Skenderis, “Weyl anomaly for Wilson surfaces,” *JHEP* **06** (1999) 12, [hep-th/9905163](#).
- [33] A. Gustavsson, “On the Weyl anomaly of Wilson surfaces,” *JHEP* **12** (2003) 59, [hep-th/0310037](#).
- [34] I. S. Gradshteyn and I. M. Ryzhik, *Table of integrals, series, and products*. Academic press, 2014.
- [35] R. C. Myers and A. Singh, “Entanglement entropy for singular surfaces,” *JHEP* **09** (2012) 13, [arXiv:1206.5225](#).
- [36] P. Bueno, H. Casini, and W. Witczak-Krempa, “Generalizing the entanglement entropy of singular regions in conformal field theories,” *JHEP* **08** (2019) 069, [arXiv:1904.11495](#).
- [37] I. R. Klebanov, T. Nishioka, S. S. Pufu, and B. R. Safdi, “On shape dependence and RG flow of entanglement entropy,” *JHEP* **07** (2012) 001, [arXiv:1204.4160](#).
- [38] J. M. Maldacena, “The Large N limit of superconformal field theories and supergravity,” *Int. J. Theor. Phys.* **38** (1999) 1113–1133, [hep-th/9711200](#).
- [39] G. P. Korchemsky, “Asymptotics of the Altarelli-Parisi-Lipatov Evolution Kernels of Parton Distributions,” *Mod. Phys. Lett. A* **4** (1989) 1257–1276.
- [40] G. P. Korchemsky and G. Marchesini, “Structure function for large x and renormalization of Wilson loop,” *Nucl. Phys. B* **406** (1993) 225–258, [hep-ph/9210281](#).
- [41] S. S. Gubser, I. R. Klebanov, and A. M. Polyakov, “A semiclassical limit of the gauge/string correspondence,” *Nucl. Phys. B* **636** (2002) 99–114, [hep-th/0204051](#).
- [42] Z. Bern, L. J. Dixon, and V. A. Smirnov, “Iteration of planar amplitudes in maximally supersymmetric Yang-Mills theory at three loops and beyond,” *Phys. Rev. D* **72** (2005) 085001, [hep-th/0505205](#).
- [43] L. F. Alday and J. Maldacena, “Comments on gluon scattering amplitudes via AdS/CFT ,” *JHEP* **11** (2007) 068, [arXiv:0710.1060](#).
- [44] J. Bhattacharya and A. E. Lipstein, “6d dual conformal symmetry and minimal volumes in AdS,” *JHEP* **12** (2016) 105, [arXiv:1611.02179](#).
- [45] J. L. Cardy and D. C. Lewellen, “Bulk and boundary operators in conformal field theory,” *Phys. Lett. B* **259** (1991) 274–278.
- [46] D. McAvity and H. Osborn, “Conformal field theories near a boundary in general dimensions,” *Nucl. Phys. B* **455** (1995) 522–576, [cond-mat/9505127](#).
- [47] P. Liendo, L. Rastelli, and B. C. van Rees, “The bootstrap program for boundary CFT_d ,” *JHEP* **07** (2013) 113, [arXiv:1210.4258](#).
- [48] D. Gaiotto, D. Mazáč, and M. F. Paulos, “Bootstrapping the 3d Ising twist defect,” *JHEP* **03** (2014) 100, [arXiv:1310.5078](#).

- [49] M. Billò, V. Gonçalves, E. Lauria, and M. Meineri, “Defects in conformal field theory,” *JHEP* **04** (2016) 091, [arXiv:1601.02883](#).
- [50] A. Antunes, “Conformal bootstrap near the edge,” *JHEP* **10** (2021) 057, [arXiv:2103.03132](#).
- [51] B. Fiol, E. Gerchkovitz, and Z. Komargodski, “Exact bremsstrahlung function in $\mathcal{N} = 2$ superconformal field theories,” *Phys. Rev. Lett.* **116** no. 8, (2016) 081601, [arXiv:1510.01332](#).
- [52] L. Bianchi, M. Preti, and E. Vescovi, “Exact Bremsstrahlung functions in ABJM theory,” *JHEP* **07** (2018) 060, [arXiv:1802.07726](#).
- [53] N. Drukker, D. Martelli, and I. Shamir, “The energy-momentum multiplet of supersymmetric defect field theories,” *JHEP* **08** (2017) 010, [arXiv:1701.04323](#).
- [54] N. Drukker, I. Shamir, and C. Vergu, “Defect multiplets of $\mathcal{N} = 1$ supersymmetry in 4d,” *JHEP* **01** (2018) 034, [arXiv:1711.03455](#).
- [55] L. Bianchi, M. Lemos, and M. Meineri, “Line defects and radiation in $\mathcal{N} = 2$ conformal theories,” *Phys. Rev. Lett.* **121** no. 14, (2018) 141601, [arXiv:1805.04111](#).
- [56] L. Bianchi and M. Lemos, “Superconformal surfaces in four dimensions,” *JHEP* **06** (2020) 056, [arXiv:1911.05082](#).
- [57] L. Bianchi, M. Meineri, R. C. Myers, and M. Smolkin, “Rényi entropy and conformal defects,” *JHEP* **07** (2016) 76, [arXiv:1511.06713](#).
- [58] N. B. Agmon and Y. Wang, “Classifying superconformal defects in diverse dimensions part I: superconformal lines,” [arXiv:2009.06650](#).
- [59] N. Drukker, S. Giombi, R. Ricci, and D. Trancanelli, “More supersymmetric Wilson loops,” *Phys. Rev. D* **76** (2007) 107703, [arXiv:0704.2237](#).
- [60] N. Drukker, S. Giombi, R. Ricci, and D. Trancanelli, “Wilson loops: From four-dimensional SYM to two-dimensional YM,” *Phys. Rev. D* **77** (2008) 047901, [arXiv:0707.2699](#).
- [61] N. Drukker, S. Giombi, R. Ricci, and D. Trancanelli, “Supersymmetric Wilson loops on S^3 ,” *JHEP* **05** (2008) 017, [arXiv:0711.3226](#).
- [62] V. Pestun, “Localization of the four-dimensional $\mathcal{N} = 4$ SYM to a two-sphere and 1/8 BPS Wilson loops,” *JHEP* **12** (2012) 067, [arXiv:0906.0638](#).
- [63] N. Drukker and B. Fiol, “All-genus calculation of Wilson loops using D-branes,” *JHEP* **02** (2005) 010, [hep-th/0501109](#).
- [64] S. Yamaguchi, “Wilson loops of anti-symmetric representation and D5-branes,” *JHEP* **05** (2006) 037, [hep-th/0603208](#).
- [65] J. Gomis and F. Passerini, “Holographic Wilson loops,” *JHEP* **08** (2006) 074, [hep-th/0604007](#).
- [66] S. A. Hartnoll and S. P. Kumar, “Higher rank Wilson loops from a matrix model,” *JHEP* **08** (2006) 026, [hep-th/0605027](#).
- [67] E. D’Hoker, J. Estes, and M. Gutperle, “Gravity duals of half-BPS Wilson loops,” *JHEP* **06** (2007) 063, [arXiv:0705.1004](#).
- [68] X. Chen-Lin, “Symmetric Wilson Loops beyond leading order,” *SciPost Phys.* **1** no. 2, (2016) 013, [arXiv:1610.02914](#).
- [69] B. Fiol and G. Torrents, “Exact results for Wilson loops in arbitrary representations,” *JHEP* **01** (2014) 020, [arXiv:1311.2058](#).

- [70] B. Fiol, J. Martínez-Montoya, and A. Rios Fukelman, “Wilson loops in terms of color invariants,” *JHEP* **05** (2019) 202, [arXiv:1812.06890](#).
- [71] S. Giombi, R. Roiban, and A. A. Tseytlin, “Half-BPS Wilson loop and AdS_2/CFT_1 ,” *Nucl. Phys.* **B922** (2017) 499–527, [arXiv:1706.00756](#).
- [72] P. Liendo, C. Meneghelli, and V. Mitev, “Bootstrapping the half-BPS line defect,” *JHEP* **10** (2018) 077, [arXiv:1806.01862](#).
- [73] P. Ferrero and C. Meneghelli, “Bootstrapping the half-BPS line defect CFT in $\mathcal{N} = 4$ supersymmetric Yang-Mills theory at strong coupling,” *Phys. Rev. D* **104** no. 8, (2021) L081703, [arXiv:2103.10440](#).
- [74] A. Cavaglià, N. Gromov, J. Julius, and M. Preti, “Integrability and conformal bootstrap: One dimensional defect conformal field theory,” *Phys. Rev. D* **105** no. 2, (2022) L021902, [arXiv:2107.08510](#).
- [75] A. Cavaglià, N. Gromov, J. Julius, and M. Preti, “Bootstrability in defect CFT: integrated correlators and sharper bounds,” [arXiv:2203.09556](#).
- [76] N. Drukker, Z. Kong, and G. Sakkas, “Broken R-symmetry and defect conformal manifolds,” [arXiv:2203.17157](#).
- [77] M. Kruczenski, R. Roiban, A. Tirziu, and A. A. Tseytlin, “Strong-coupling expansion of cusp anomaly and gluon amplitudes from quantum open strings in $AdS_5 \times S^5$,” *Nucl. Phys. B* **791** (2008) 93–124, [arXiv:0707.4254](#).
- [78] E. Sezgin and P. Sundell, “Massless higher spins and holography,” *Nucl. Phys. B* **644** (2002) 303–370, [hep-th/0205131](#). [Erratum: *Nucl.Phys.B* 660, 403–403 (2003)].
- [79] S. A. Hartnoll and C. Nunez, “Rotating membranes on G_2 -manifolds, logarithmic anomalous dimensions and $\mathcal{N} = 1$ duality,” *JHEP* **02** (2003) 049, [hep-th/0210218](#).